PANDORA project: photo-nuclear reactions for understanding extragalactic propagation of ultra-high-energy cosmic rays

Atsushi Tamii

Research Center for Nuclear Physics (RCNP)
Osaka University, Japan

for the PANDORA collaboration

NEWS Colloquium
August 31, 2020 at RCNP

Ultra-High-Energy Cosmic Rays (UHECRs)
production - propagation - observation

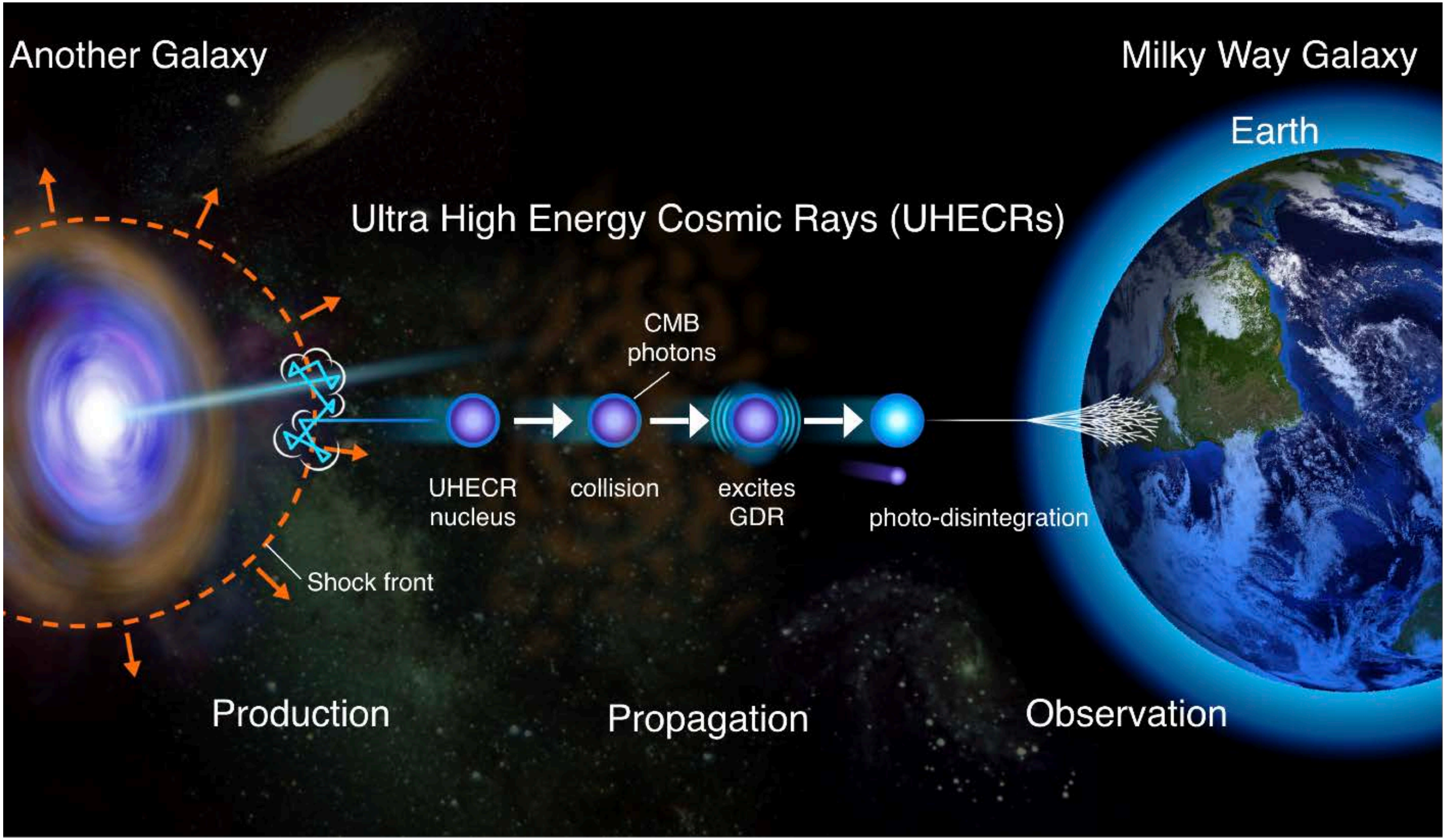

Outline

I. Ultra-high-energy Cosmic Rays (UHECRs)

II. Observatories

III. Mass Composition and Anisotropy

IV. Energy Loss Process in Space Propagation

V. PANDORA project

UHECRs

Primary Cosmic Ray Flux and Composition

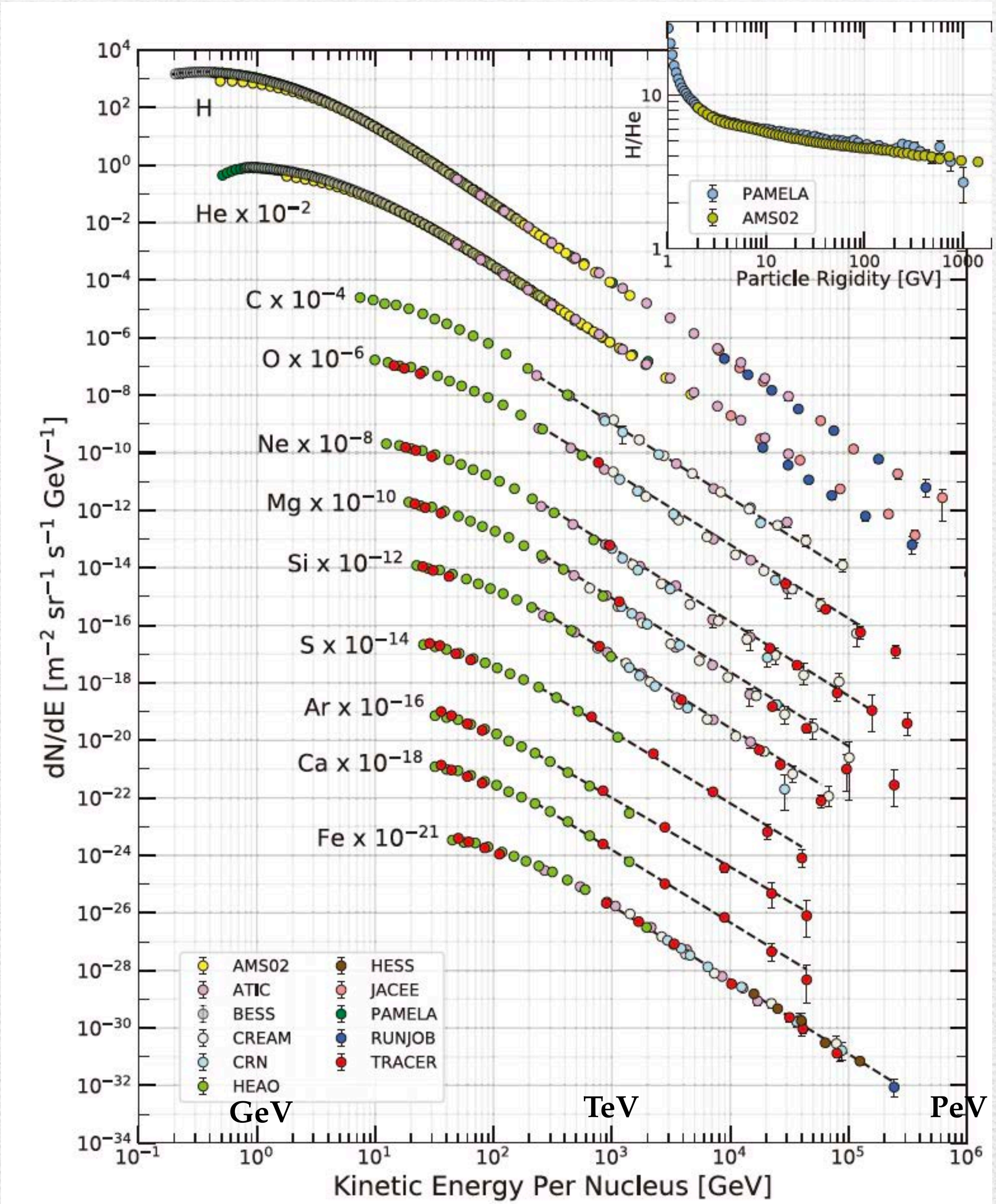

Z	Element	F	Z	Element	F
1	H	550	13–14	Al-Si	0.19
2	He	34	15–16	P-S	0.03
3–5	Li-B	0.40	17–18	Cl-Ar	0.01
6–8	C-O	2.20	19–20	K-Ca	0.02
9–10	F-Ne	0.30	21–25	Sc-Mn	0.05
11–12	Na-Mg	0.22	26–28	Fe-Ni	0.12

composition relative to oxygen at 10.6 GeV/A

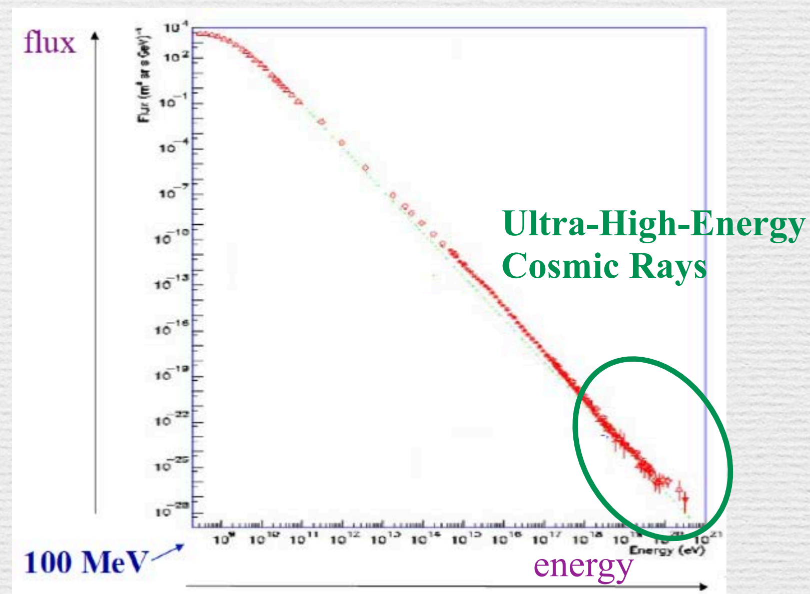

[PDG2018]

Ultra-High-Energy Cosmic Rays (UHECRs) [PDG2018]

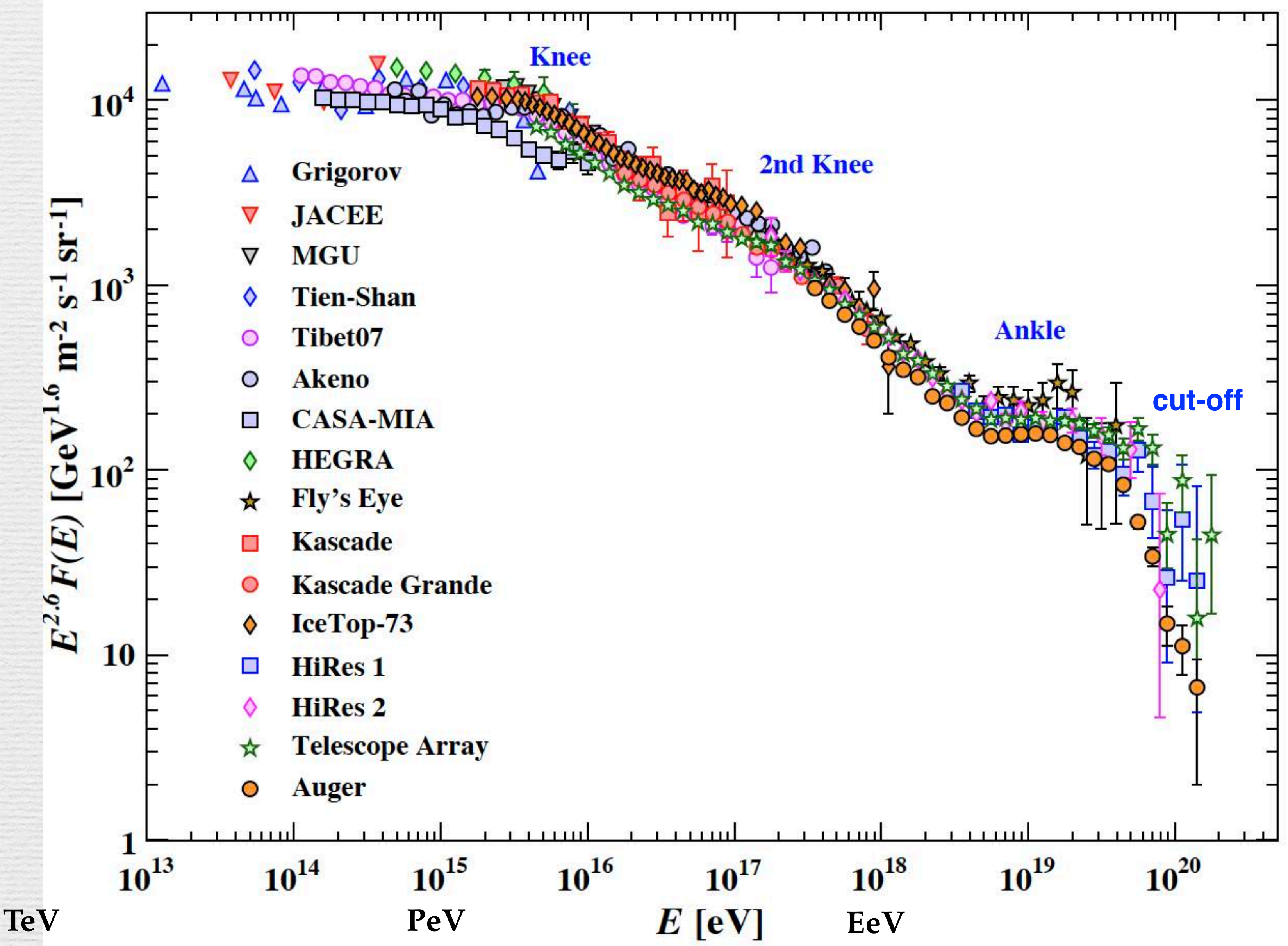

Ultra-High-Energy Cosmic Rays (UHECRs) [PDG2018]

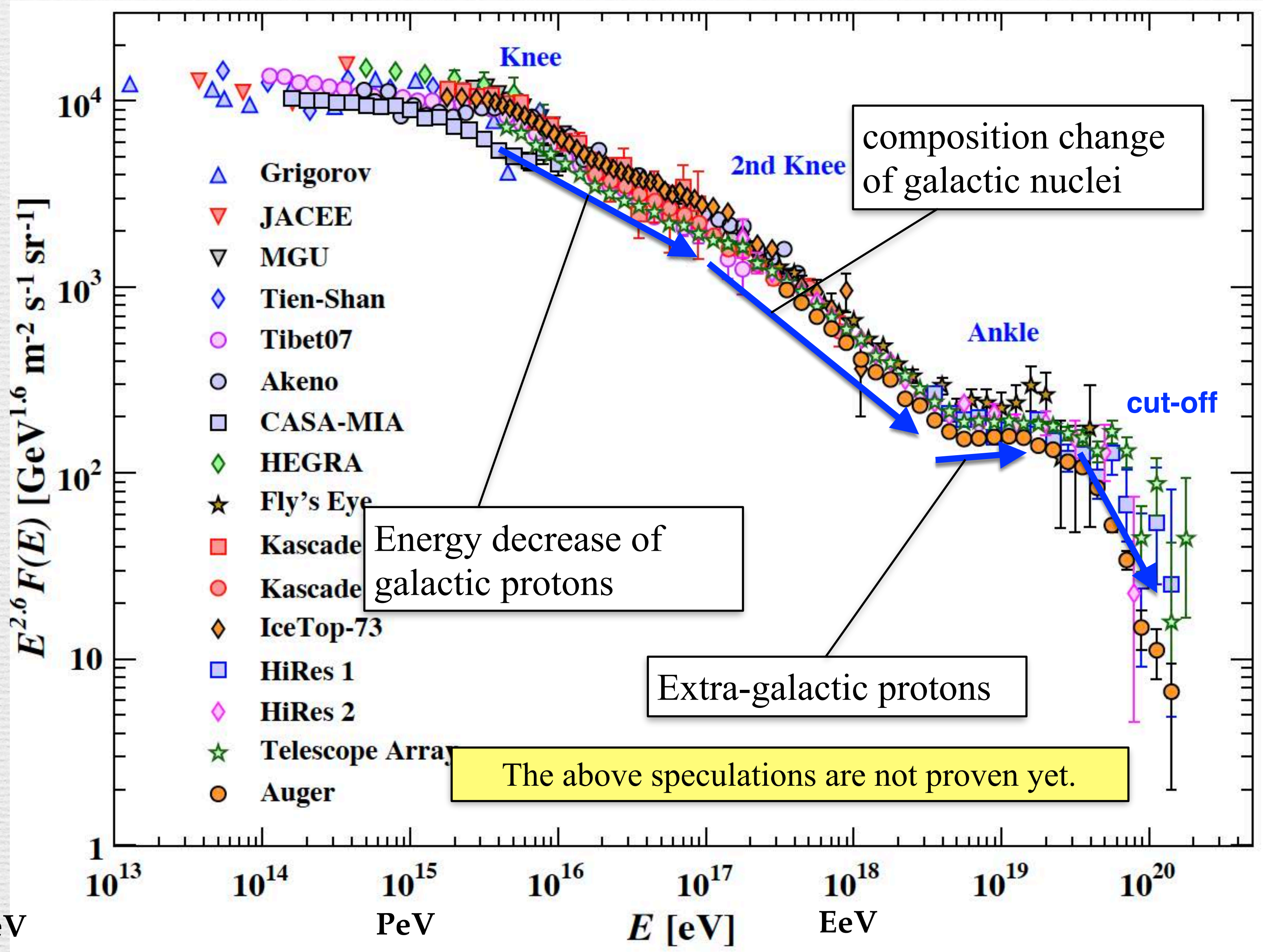

Ultra-High-Energy Cosmic Rays (UHECRs) [PDG2018]

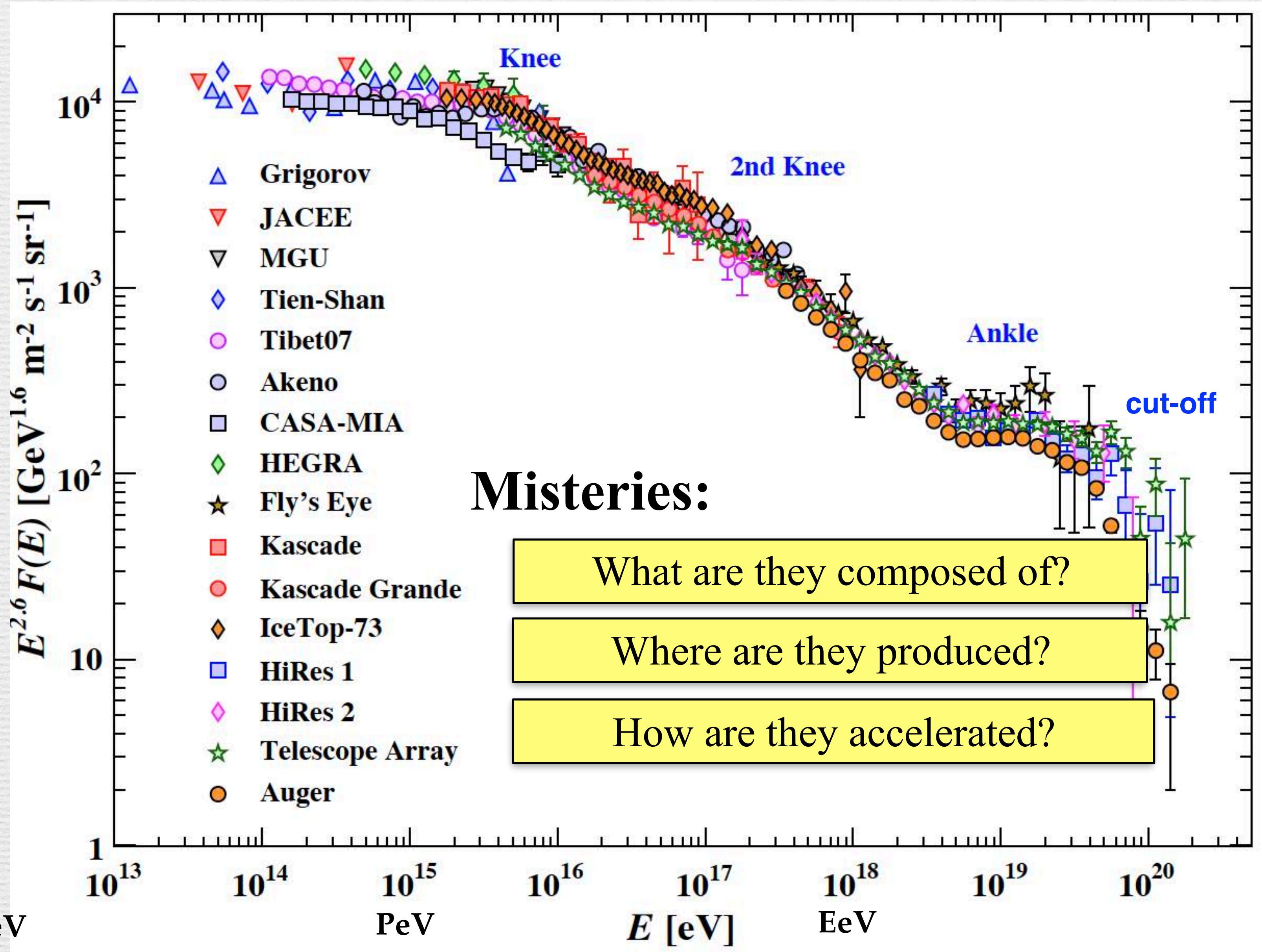

Misteries:

What are they composed of?

Where are they produced?

How are they accelerated?

UHECR Observatories

Observation of UHECRs

Extended Air Shower (EAS)

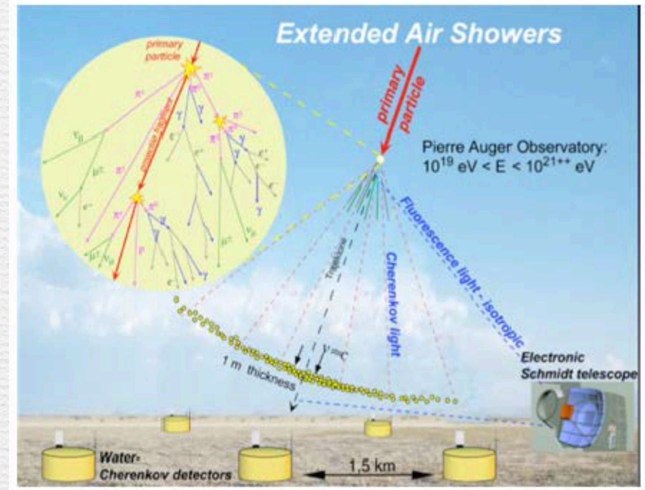

Hadronic process

primarily produces mesons (π or K)

p(A) +A → π, K, and nuclear fragments

$\pi^{\pm} \rightarrow \mu^{\pm} + \nu_{\mu}\ (\overline{\nu_{\mu}})$

$\pi^{0} \rightarrow 2\gamma$

$\gamma \rightarrow e^{+}+e^{-}$

$e^{\pm} + A \rightarrow e^{\pm}+A+\gamma$

Electromagnetic Shower

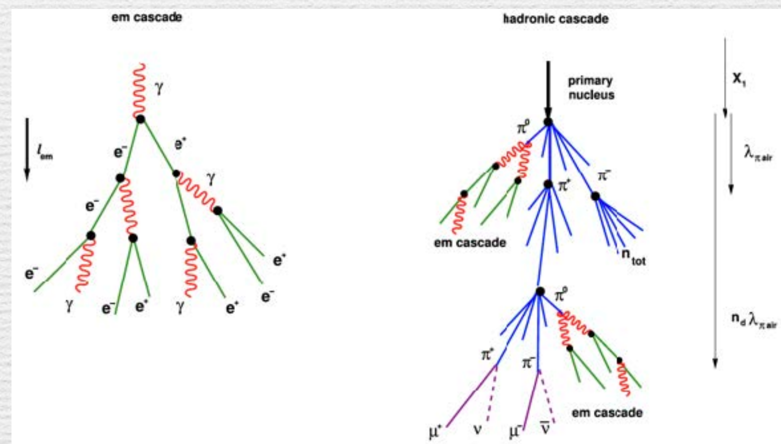

[mol18]

(RCNP →) Pierre Auger Observatory

Pierre Auger Observatory

©google map

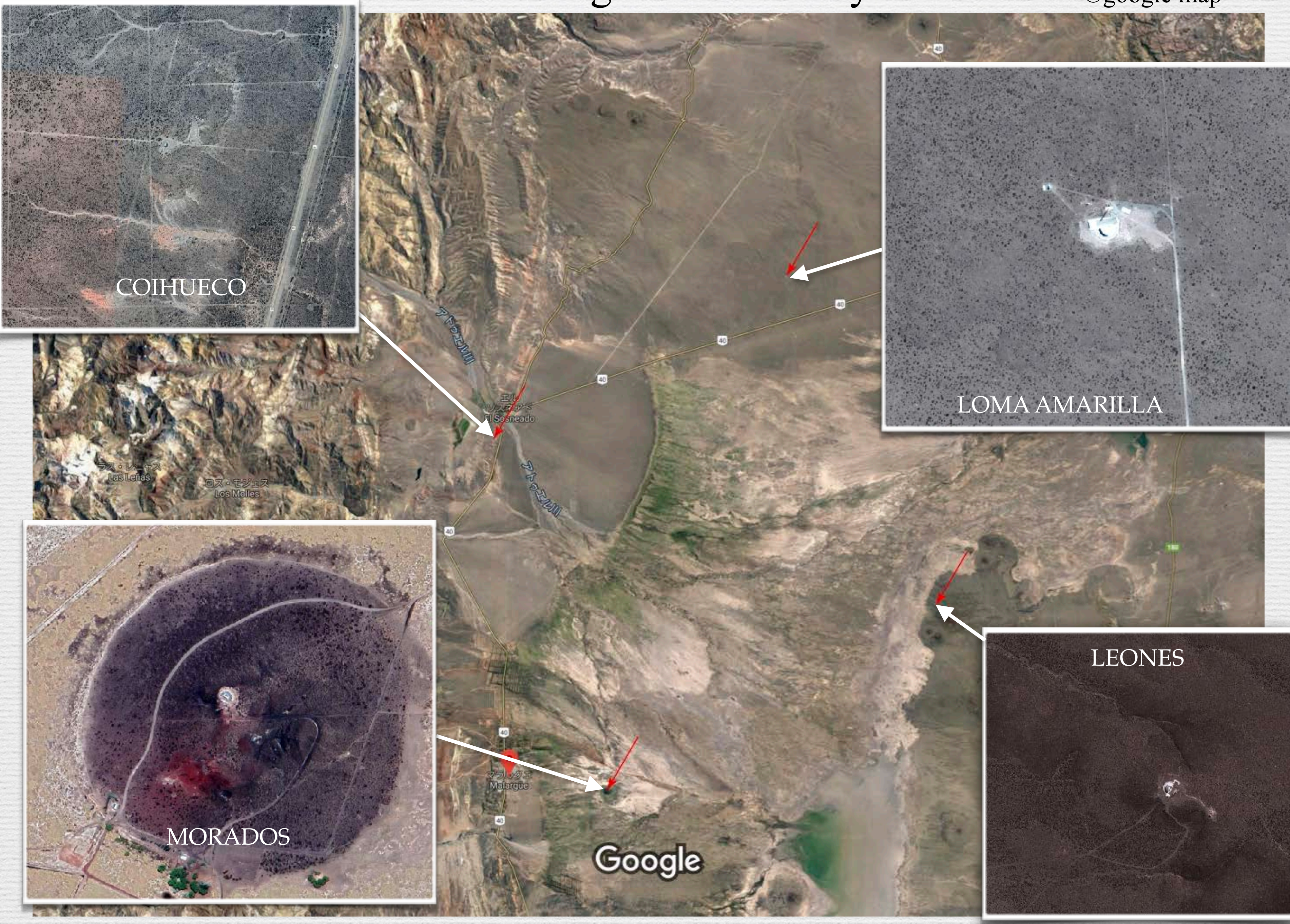

Pierre Auger Observatory

[aug15, aug04]

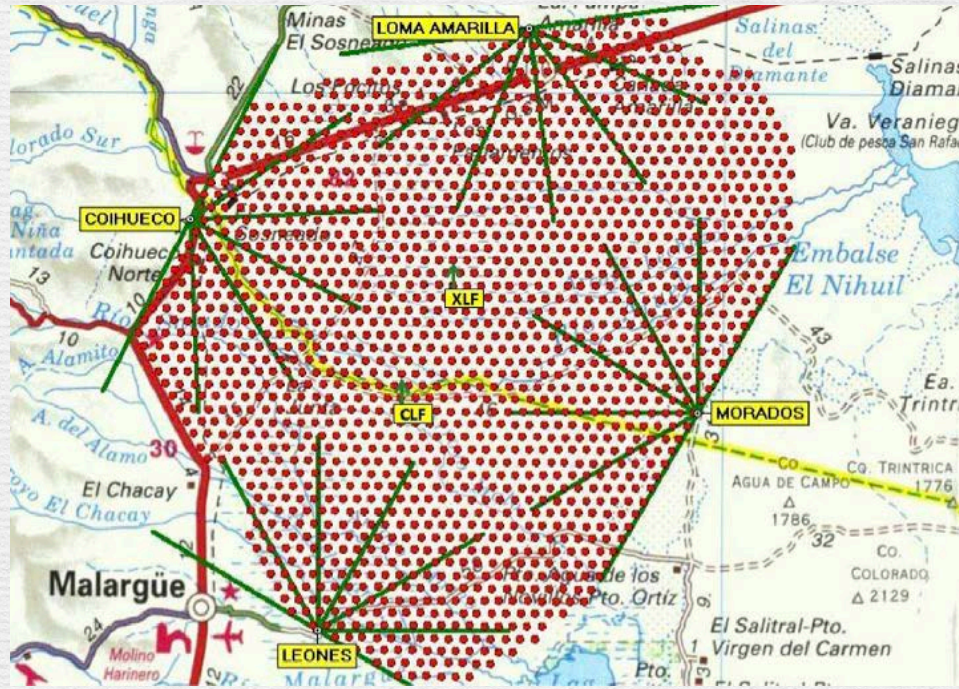

The Pampa Amarilla site (35.1°–35.5° S, 69.0°–69.6° W and 1300–1400 m asl) lies in the south of the Province of Mendoza, Argentina, close to Malargüe (pop. 18 000) and 180 km south west of San Rafael (pop. 100 000). It encompasses an area of 3100 km^2 (see Fig. 1a).

(Auger →) Telescope Array

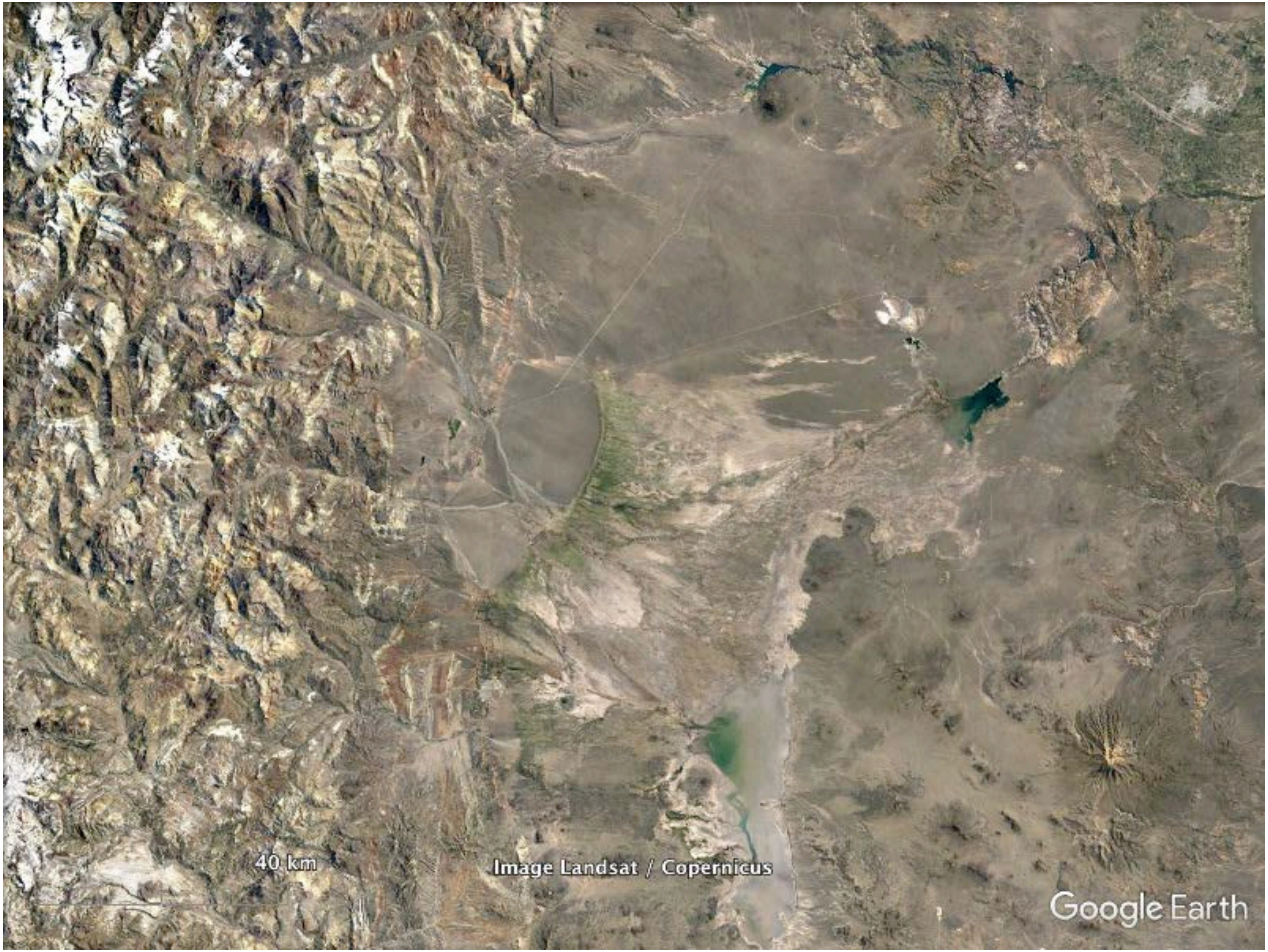

Telescope Array

[tok11, abu12,]

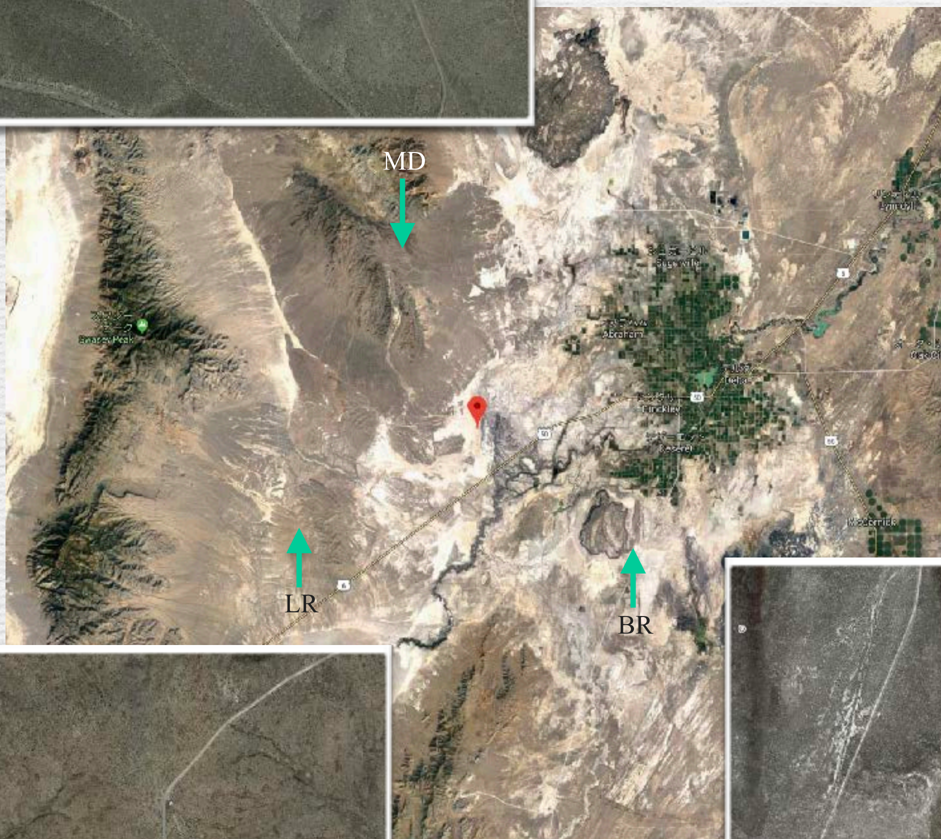

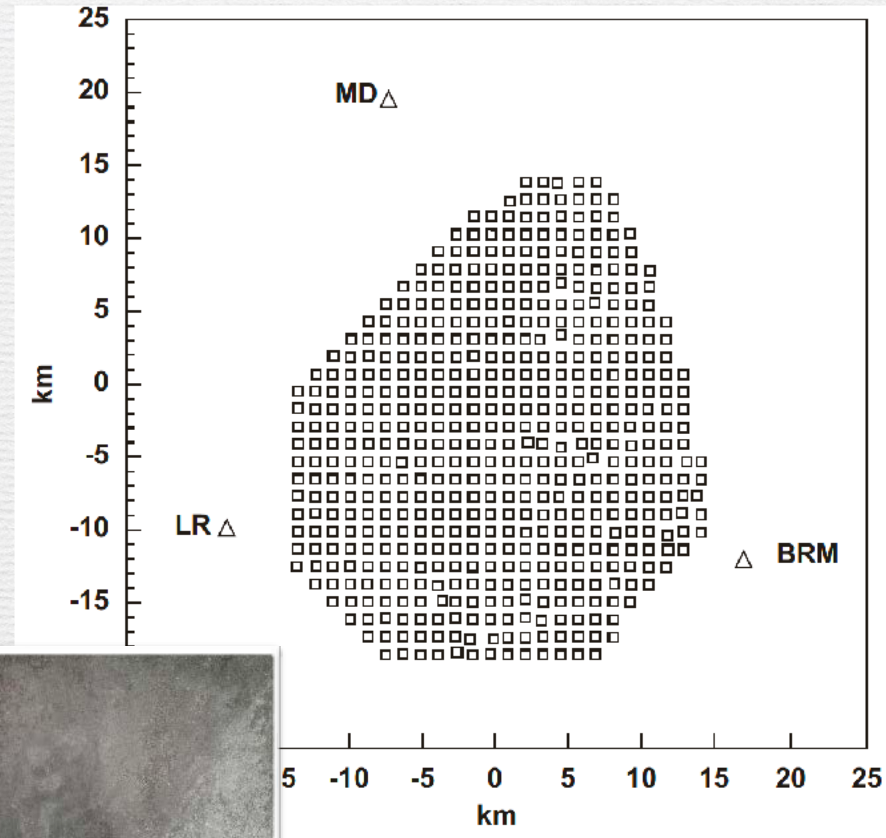

cated in the desert about 1400 m above sea level
and 112.9°W in Millard County, Utah, USA, about
of Salt Lake City. A control center to support

Pierre Auger Observatory
Surface Detectors (SDs)

[aug04]

3,000 km^2 (~60kmϕ)

1,600 water Cherenkov detectors (SD)
in a polyethylene tank

mean distance 1.5 km on triangular grid

~0.5 SD / km^2

High-purity water
in three-layers of polyolefin liner
(140+28+178μm)

10 m^2 area × 1.2 m depth

Three PMT's

Hamamatsu R5921 8″ϕ
or
Photonis XP1802 9″ϕ

FADC 40 MHz

Time recording calibrated by GPS.
(σ=7.24 ns)

100% running efficiency measured from 2004

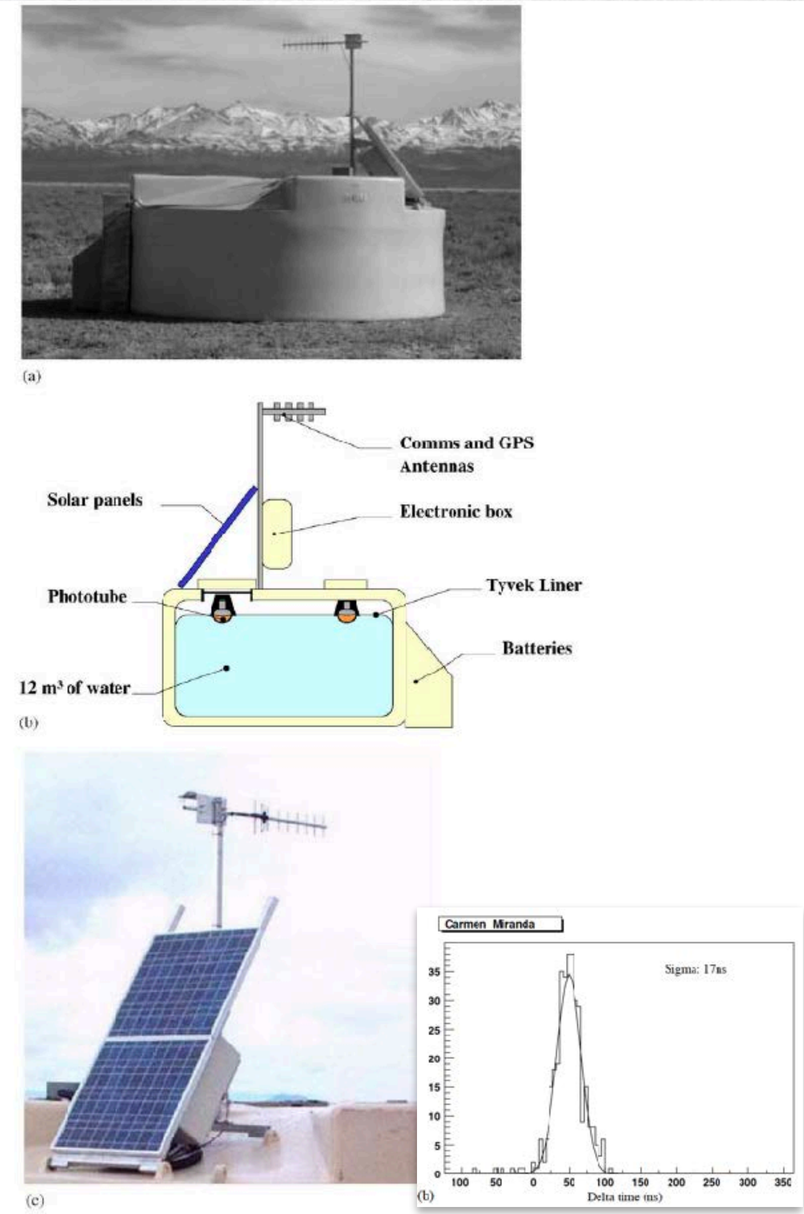

Fig. 2. (a) A photograph of an EA water tank; (b) schematic view of an EA tank; (c) the Yagi antenna and the solar power array.

Telescope Array
Surface Detectors (SDs)

[tok11, abu12,]

700 km² (~30kmϕ)

507 plastic scintillation counter of 3m²×1.2cm×2 layers

mean distance 1.2 km on square grid

~0.7 SD / km²

104 wavelength-shifting fibers

PMT 9124SA; Electron Tubes Ltd.

12bit 50 MHz FADC

Time recording calibrated by GPS.

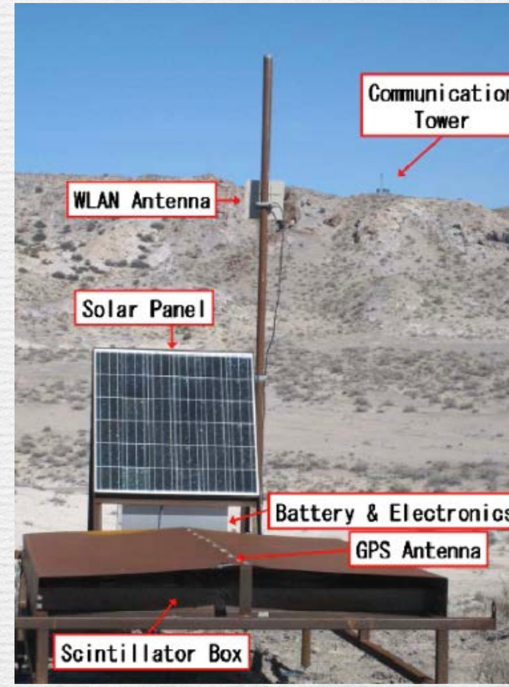

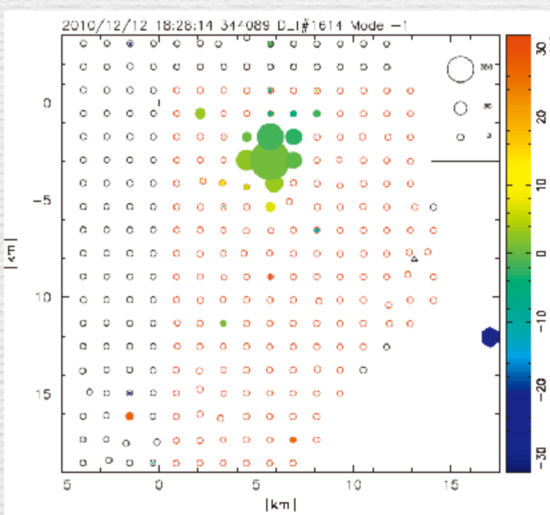

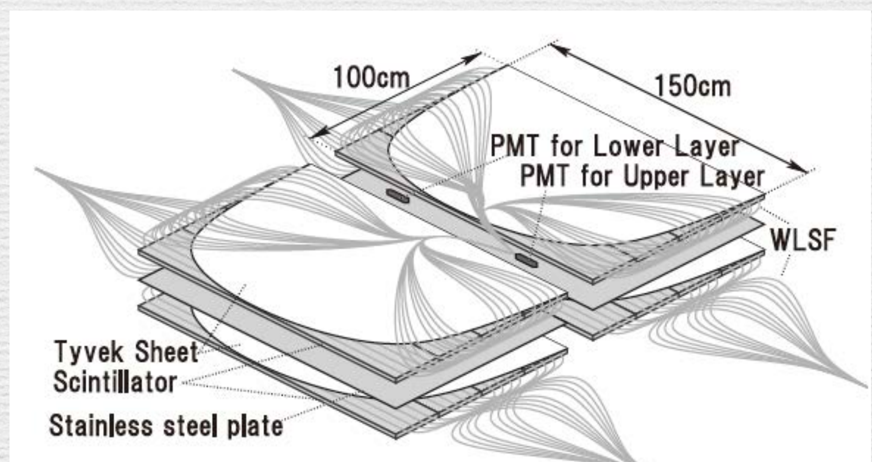

Pierre Auger Observatory
(Fluorescence Detectors) FDs

[aug15, aug04]

24 fluorescence detector telescopes at 4 sites

with spherical mirror (3.5m×3.5m)
and (440) PMT camera

30° azimuth×28.6° elevation field of view per telescope

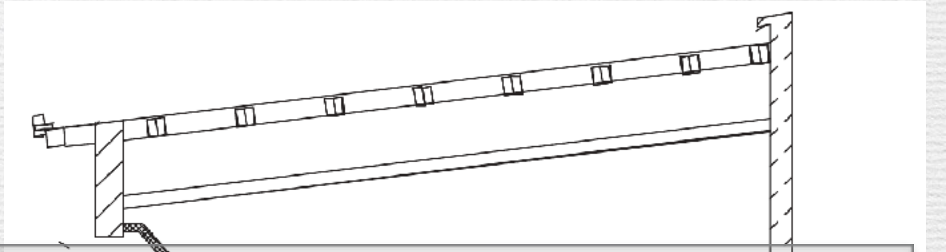

UV light 310-390 nm
fluorescence from nitrogen excited by air shower

Continuous digitization by 10MHz 12 bit ADC

100 Hz recording using sum trigger and
threshold (20μsec)

Calibrated by YAG-laser (355nm) from
CLF and XLF

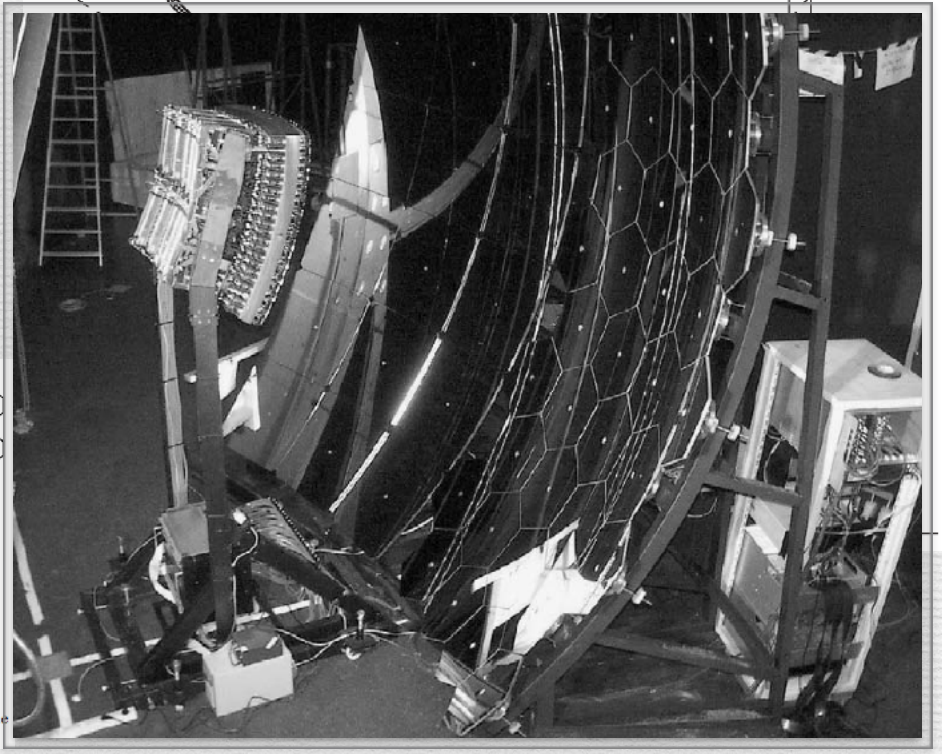

~15% running efficiency
with clear sky no moon

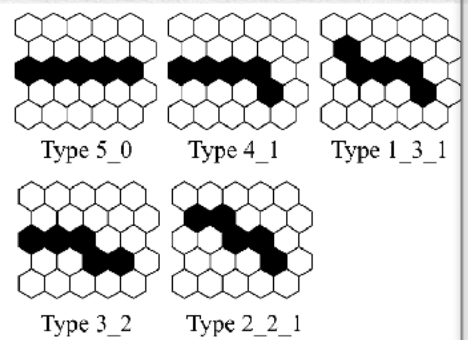

Fig. 8. Basic topological patterns of triggered pixels used in the second level trigger.

Telescope Array
FD

[tok11, abu12,]

12 fluorescence detector telescopes at 3 sites

Primary mirror (3.3mϕ) and (16×16) PMT camera

18° azimuthal 15° elevation field of view / telescope

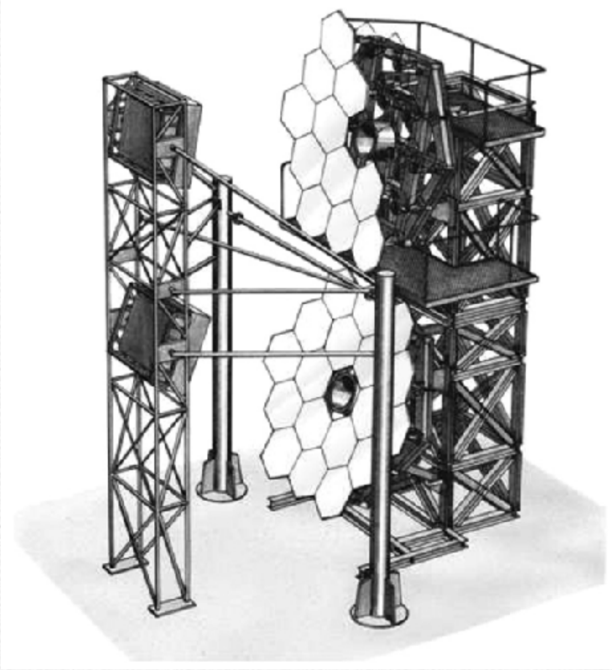

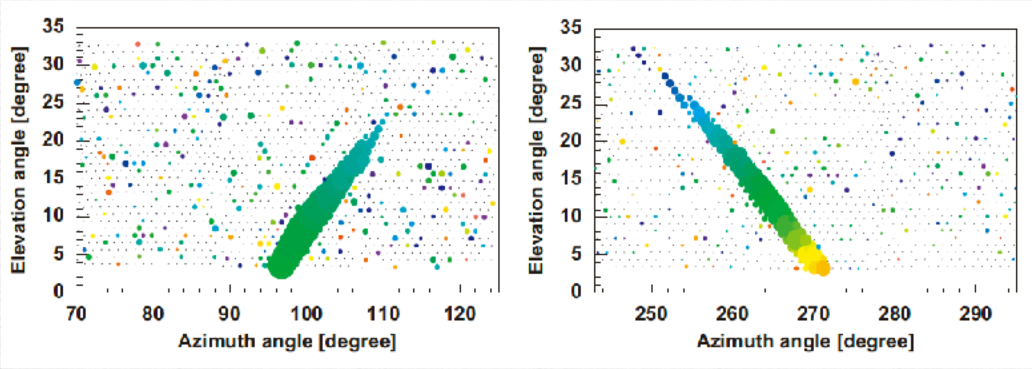

Analysis Methods

Analysis Methods
Event Reconstruction

[aug15]

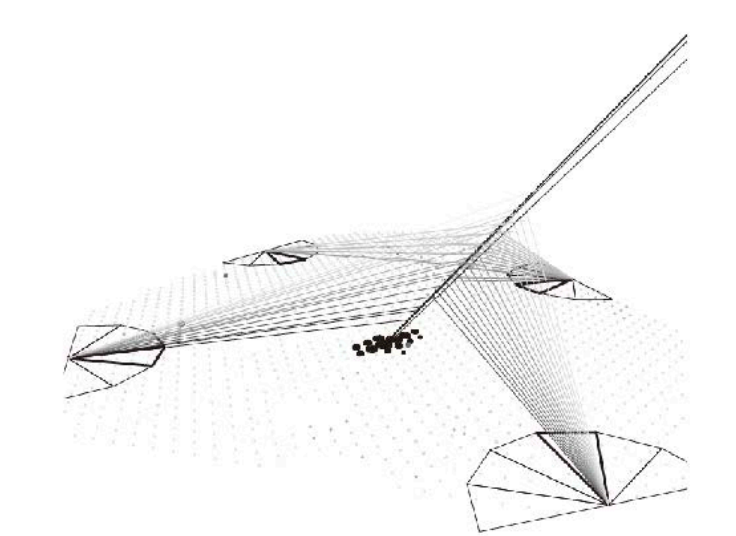

Fig. 33. Geometry reconstruction of an event observed by four telescopes and the surface detector.

Direction of CR: time difference of SD signals

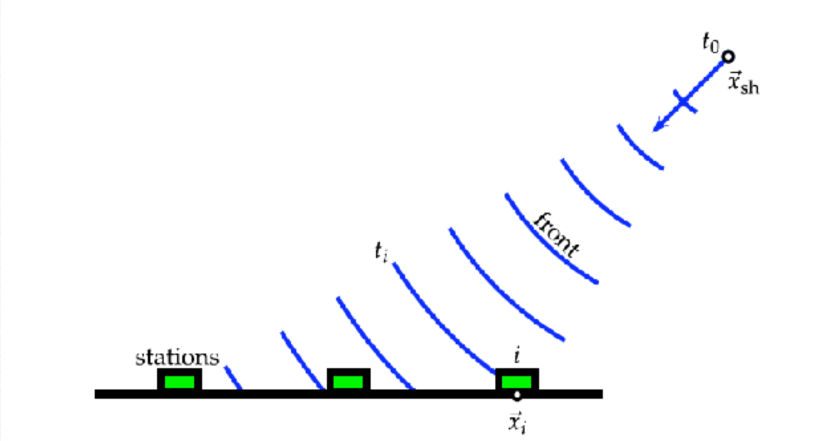

Fig. 35. Reconstruction of shower geometry: schematic representation of the evolution of the shower front.

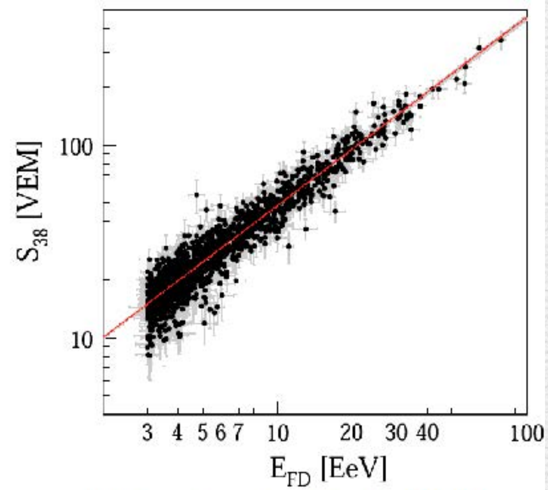

Fig. 41. Correlation between S_{38} and E_{FD} [11,122].

Absolute energy: sum of the FD signal
with correction
atmospheric attenuation
escaped events (muon, neutrino) ~10%
systematic uncertainty: 14%

The signal size (θ=38°) of SD:
correlated with CR energy, calibrated to FD.

Angular resolution ~0.5°

VEM: Vertical Equivalent Muon

Ultra-High-Energy Cosmic Rays (UHECRs)

[anc19]

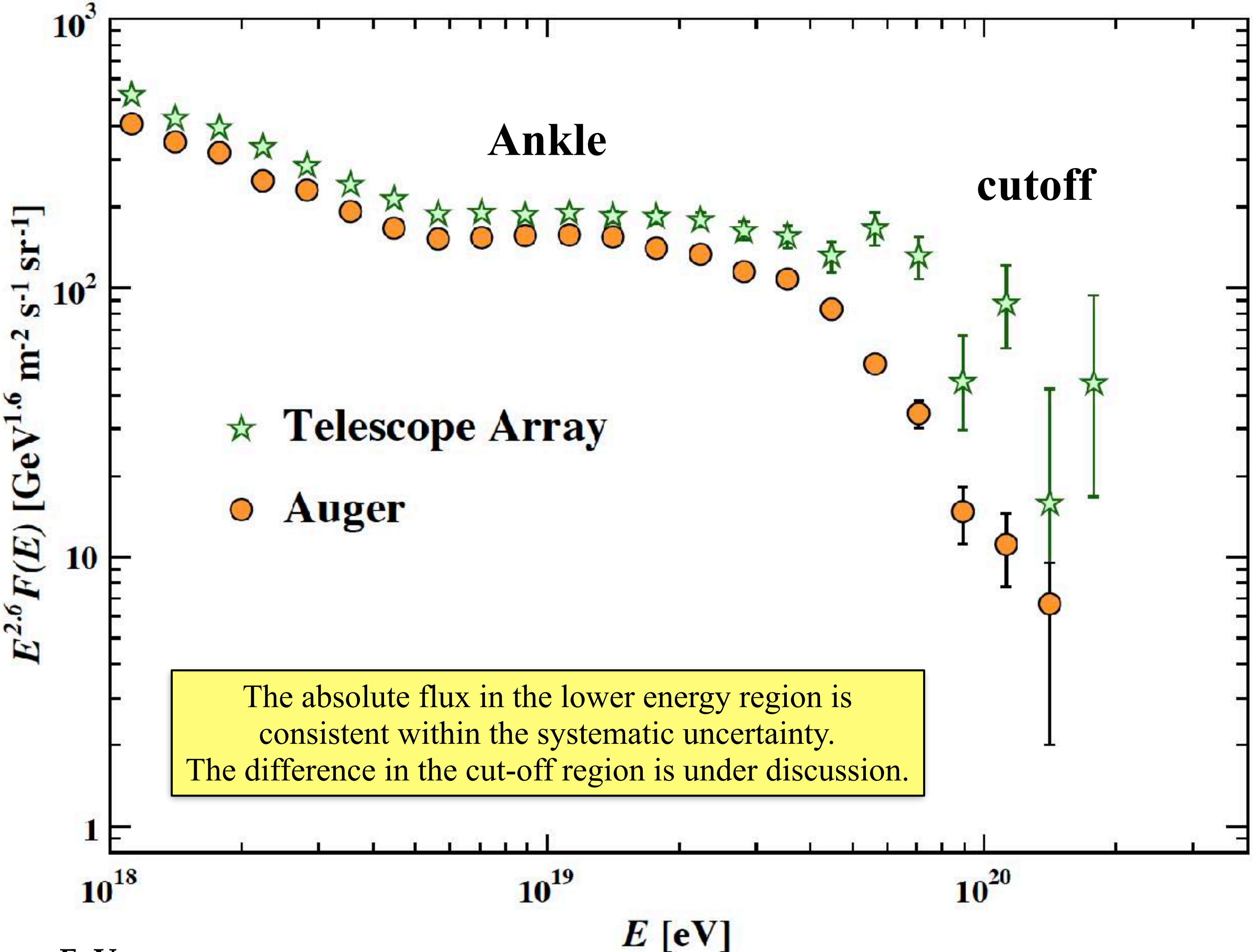

EeV

Analysis Methods (Fluorescence Detectors) FDs

[anc19]

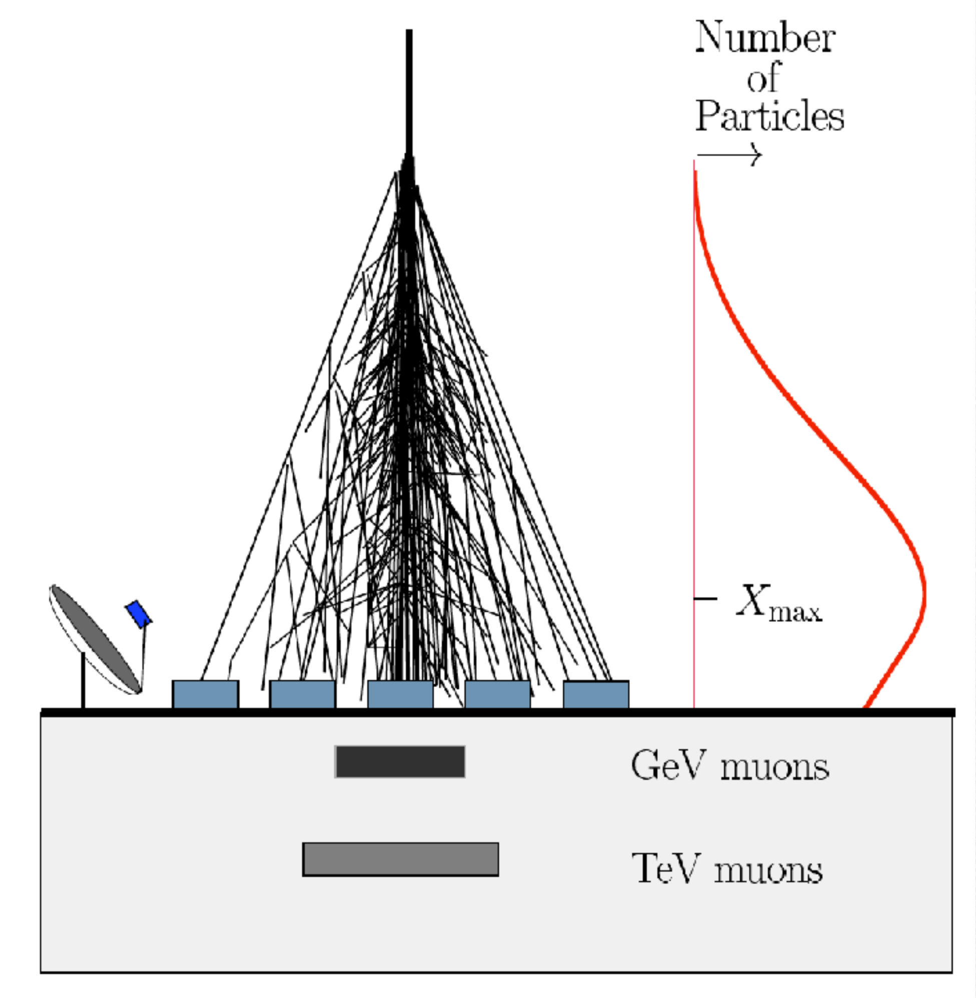

X_{max}:
atmospheric depth by FD data where the maximum number of particles is the largest.

<X_{max}>: mean of X_{max}

σ(<X_{max}>): standard deviation of X_{max}

for the events of interest

<X_{max}> and σ(<X_{max}>) are predicted to be correlated with the mass (A) of the primary CR.

The correlation depends on the hadronic shower model.

Primary beam energy is above where accelerate laboratory data are available.

$X_{\max}$ distribution predictions

[aab14]

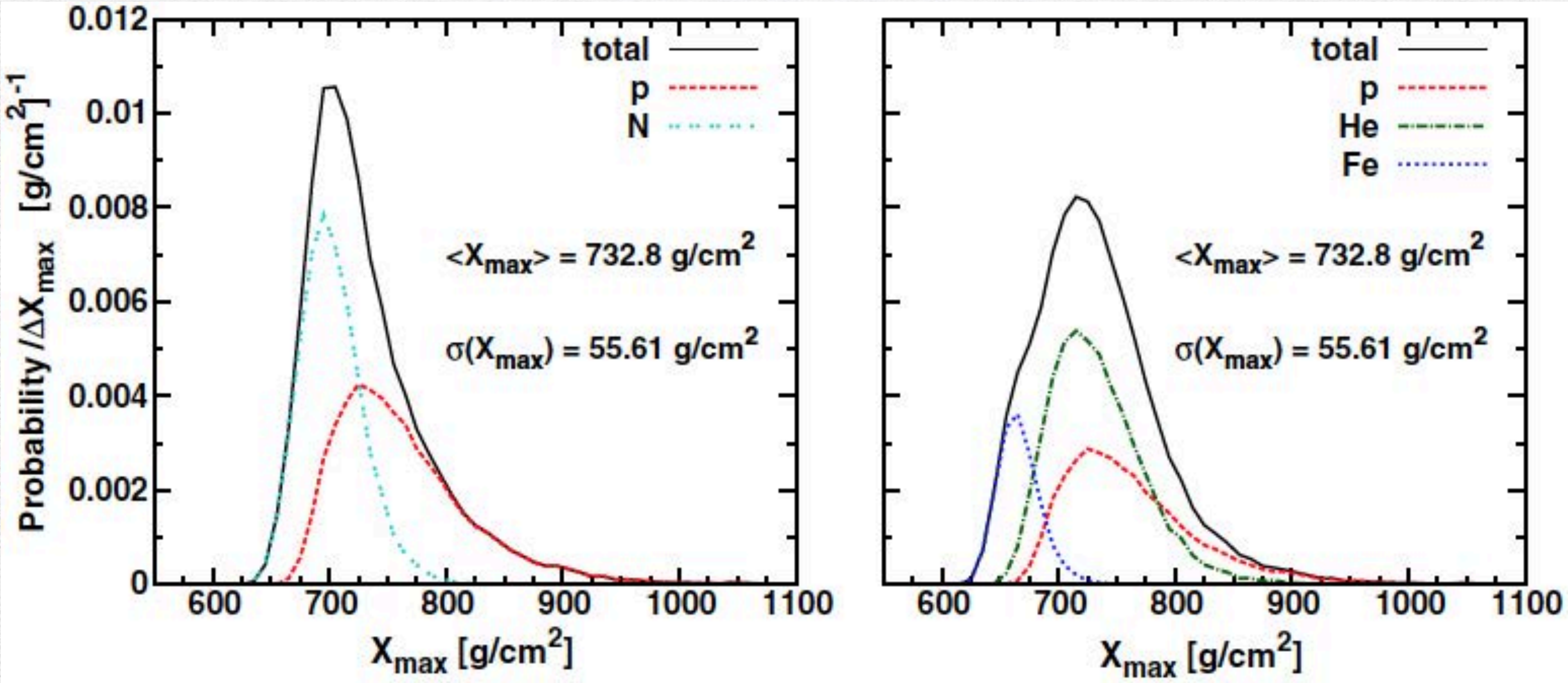

Composition

Mass Composition

[gor18]

Pierre Auger Observatory

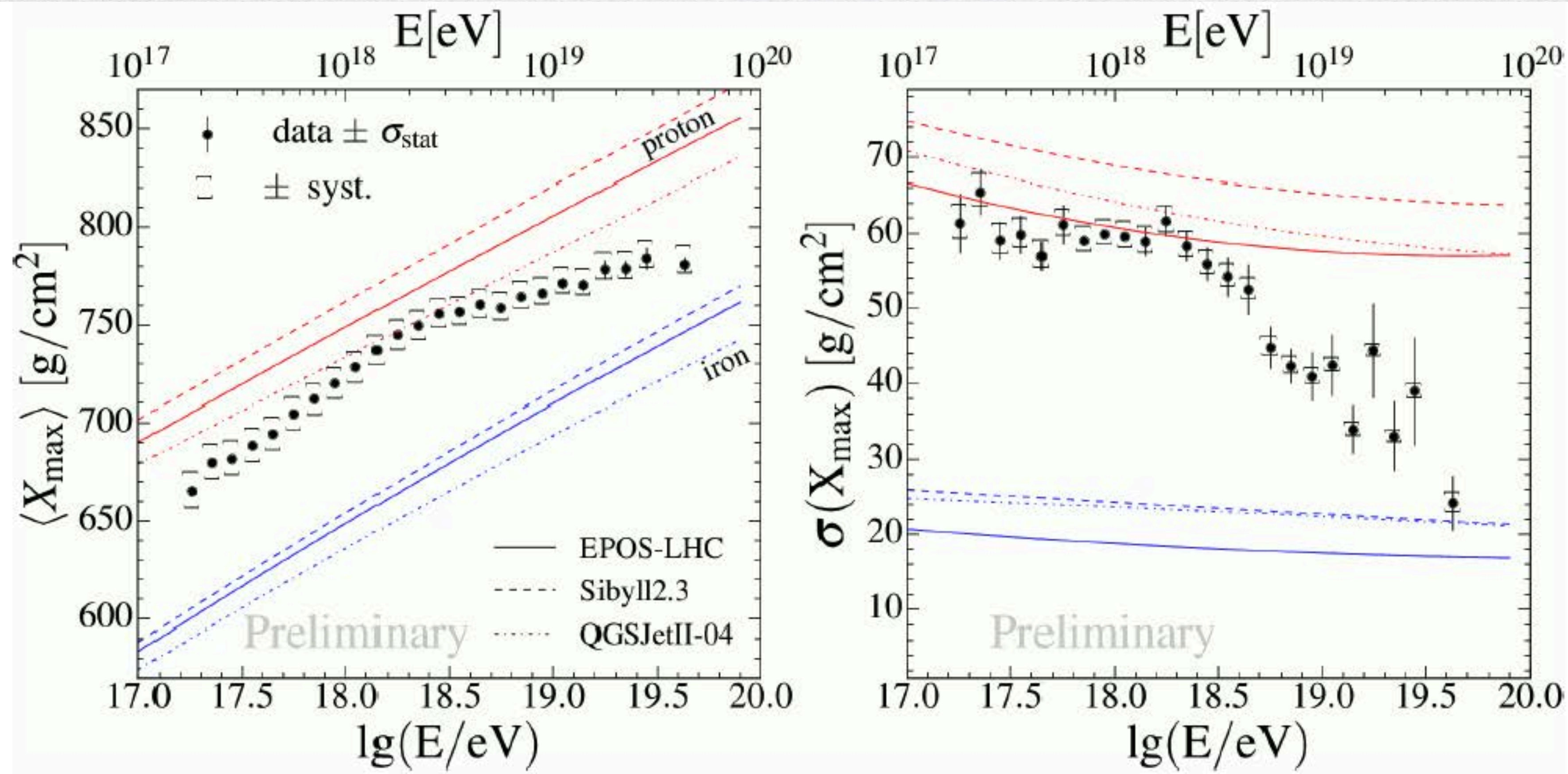

The fraction of proton increases up to $10^{18.3}$ eV and then decreases.

Composition of heavier mass nuclei are becoming dominating at the highest energy.

Mass Composition

[abb19]

Telescope Array

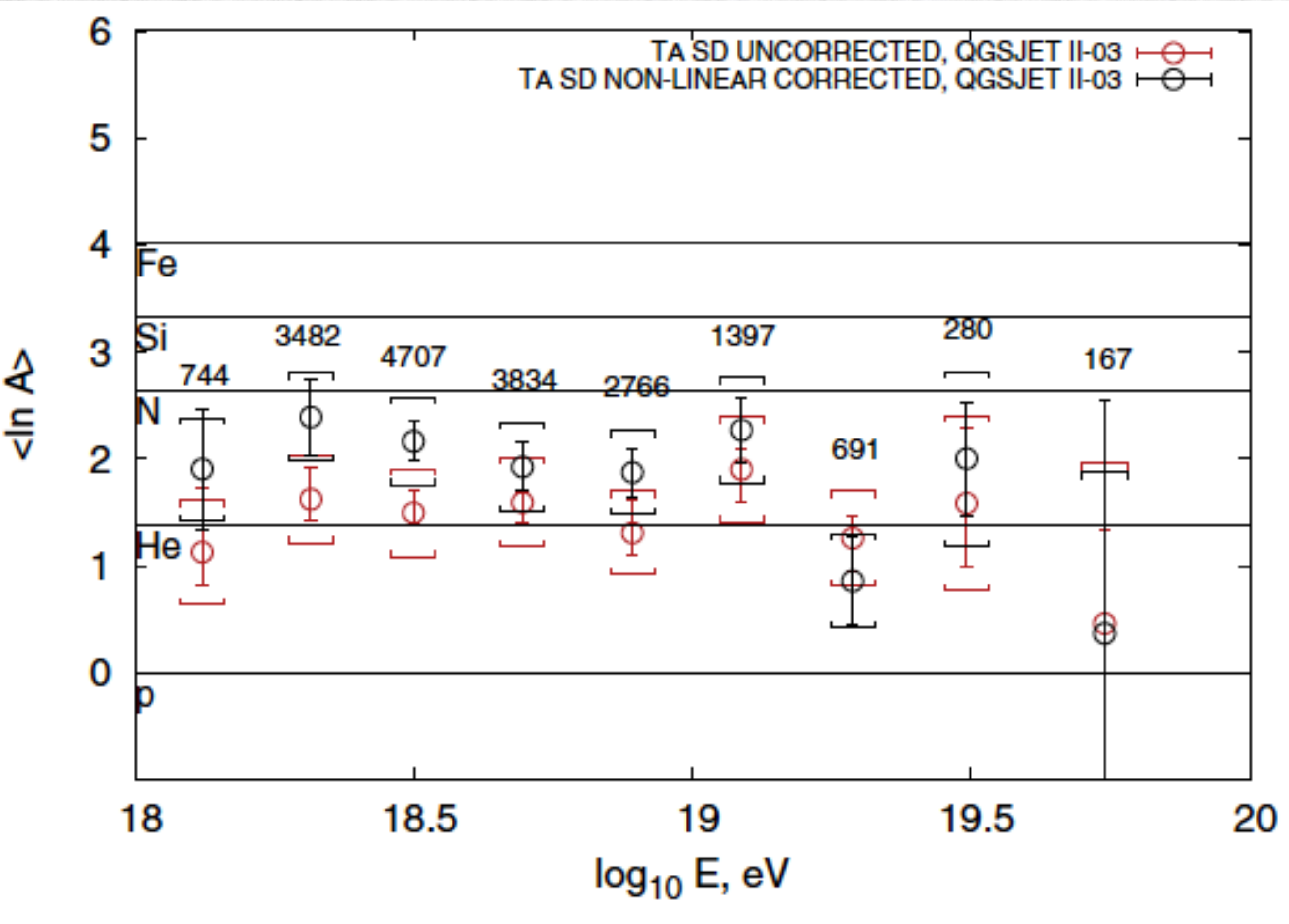

TA data also show heavier nuclei at high-energy with flatter energy dependence than Auger.

Mass Composition

[mol18]

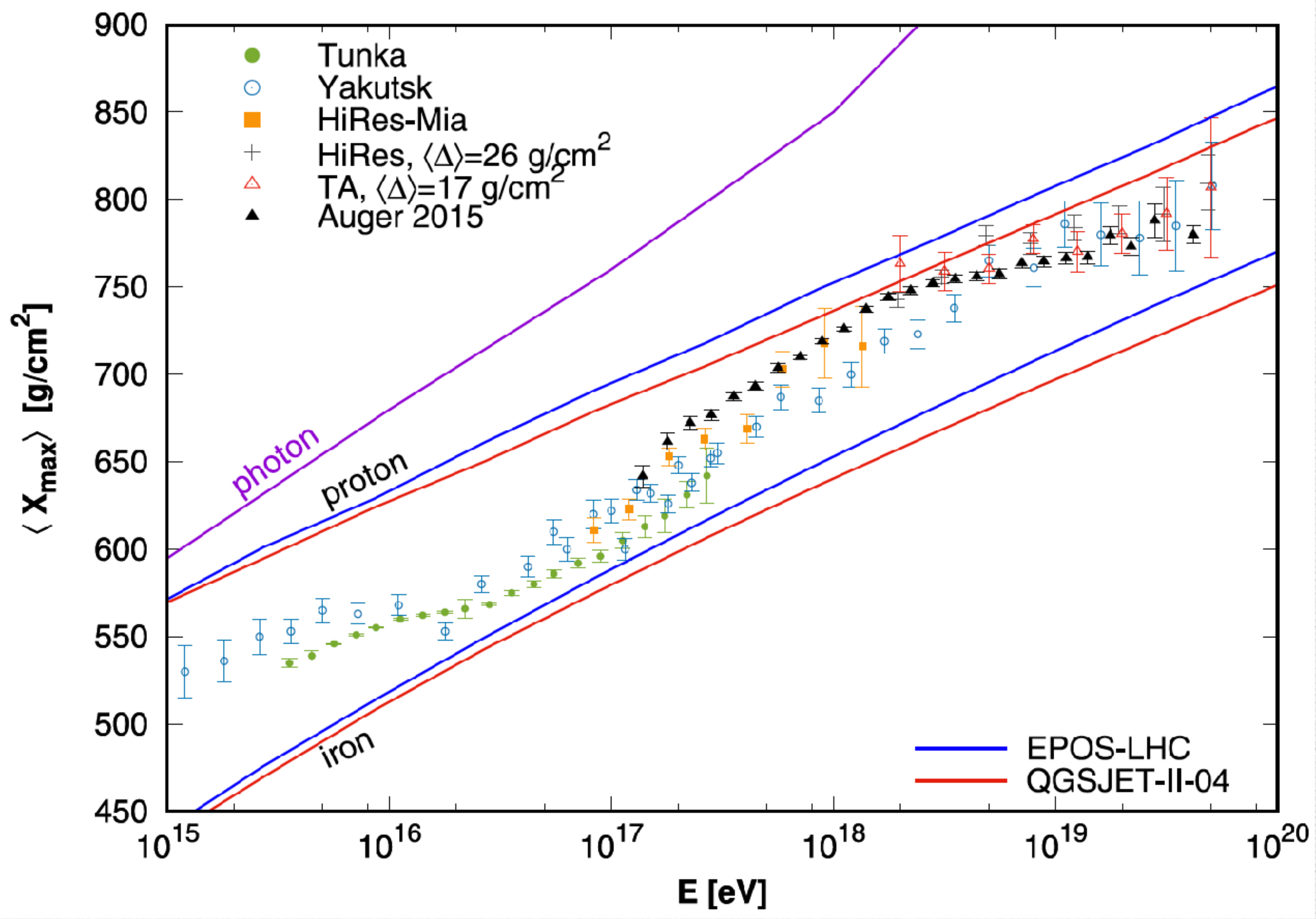

Anisotropy

Anisotropy

[aab15,aug17]

Pierre Auger Observatory

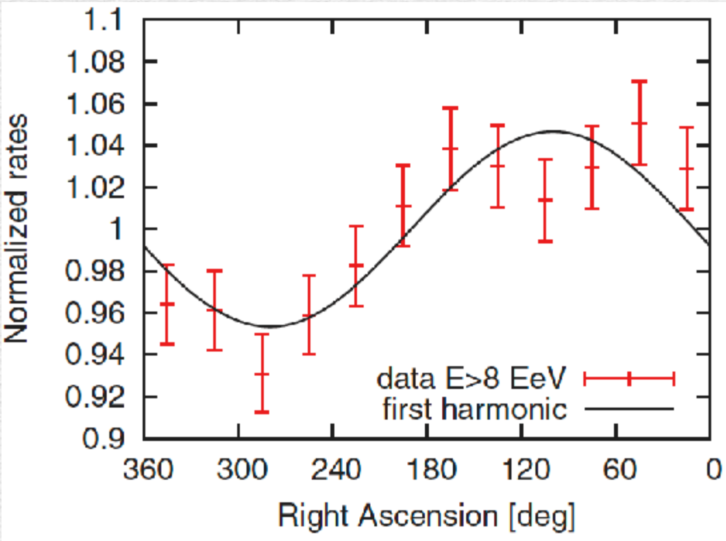

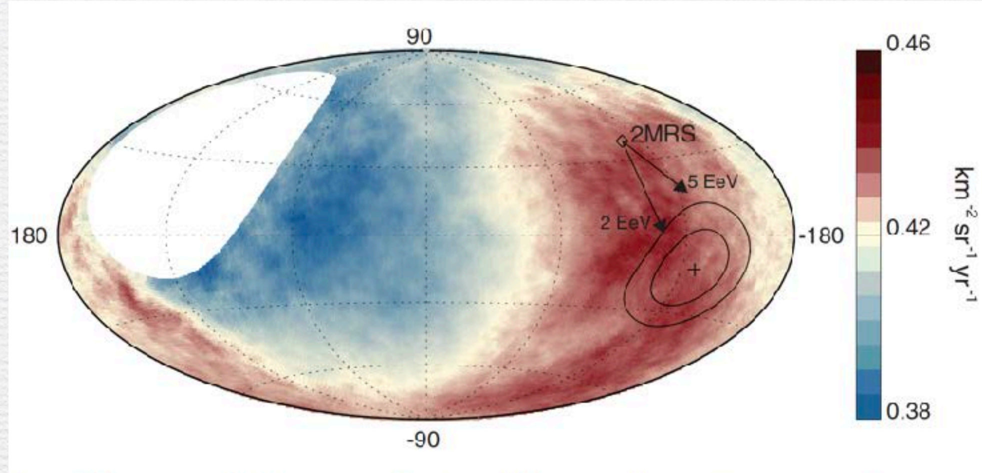

Fig. 3. Map showing the fluxes of particles in galactic coordinates. Sky map in galactic

Anisotropy by dipole fit (5.2σ)

Anisotropy after subtracting the isotropic component is analyzed.

Anisotropy is an important indicator of the sources of UHECRs and their distribution.

Anisotropy

Pierre Auger Observatory

[aab18]

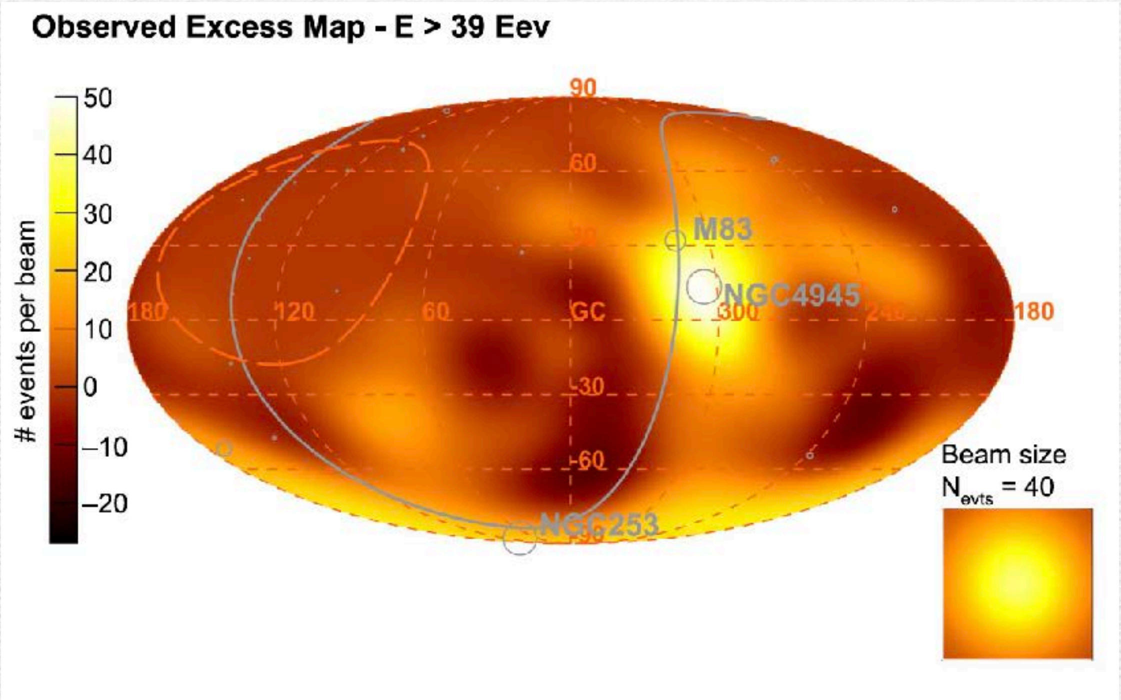

The observed anisotropy showed correlation with the distribution of SBGs (4.0σ).

SBG: star burst galaxy

γAGN: γ-active galactic nucleus

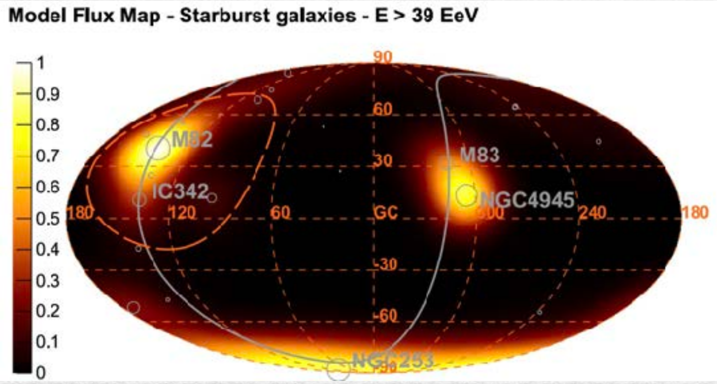

Prediction of UHECR intensity assuming SBGs as the source including attenuation in the extragalactic propagation.

Note that the region (surrounded by the dashed line) close to M82 is not covered by Auger.

Anisotropy

Pierre Auger Observatory

[aab18]

Table 1
Populations Investigated

SBGs	l (°)	b (°)	Distance[a] (Mpc)	Flux Weight (%)	Attenuated Weight: A/B/C (%)	% Contribution[b]: A/B/C (%)
NGC 253	97.4	−88	2.7	13.6	20.7/18.0/16.6	35.9/32.2/30.2
M82	141.4	40.6	3.6	18.6	24.0/22.3/21.4	0.2/0.1/0.1
NGC 4945	305.3	13.3	4	16	19.2/18.3/17.9	39.0/38.4/38.3
M83	314.6	32	4	6.3	7.6/7.2/7.1	13.1/12.9/12.9
IC 342	138.2	10.6	4	5.5	6.6/6.3/6.1	0.1/0.0/0.0
NGC 6946	95.7	11.7	5.9	3.4	3.2/3.3/3.5	0.1/0.1/0.1
NGC 2903	208.7	44.5	6.6	1.1	0.9/1.0/1.1	0.6/0.7/0.7
NGC 5055	106	74.3	7.8	0.9	0.7/0.8/0.9	0.2/0.2/0.2
NGC 3628	240.9	64.8	8.1	1.3	1.0/1.1/1.2	0.8/0.9/1.1
NGC 3627	242	64.4	8.1	1.1	0.8/0.9/1.1	0.7/0.8/0.9
NGC 4631	142.8	84.2	8.7	2.9	2.1/2.4/2.7	0.8/0.9/1.1
M51	104.9	68.6	10.3	3.6	2.3/2.8/3.3	0.3/0.4/0.5
NGC 891	140.4	−17.4	11	1.7	1.1/1.3/1.5	0.2/0.3/0.3
NGC 3556	148.3	56.3	11.4	0.7	0.4/0.6/0.6	0.0/0.0/0.0
NGC 660	141.6	−47.4	15	0.9	0.5/0.6/0.8	0.4/0.5/0.6
NGC 2146	135.7	24.9	16.3	2.6	1.3/1.7/2.0	0.0/0.0/0.0
NGC 3079	157.8	48.4	17.4	2.1	1.0/1.4/1.5	0.1/0.1/0.1
NGC 1068	172.1	−51.9	17.9	12.1	5.6/7.9/9.0	6.4/9.4/10.9
NGC 1365	238	−54.6	22.3	1.3	0.5/0.8/0.8	0.9/1.5/1.6
Arp 299	141.9	55.4	46	1.6	0.4/0.7/0.6	0.0/0.0/0.0
Arp 220	36.6	53	80	0.8	0.1/0.3/0.2	0.0/0.2/0.1
NGC 6240	20.7	27.3	105	1	0.1/0.3/0.1	0.1/0.3/0.1
Mkn 231	121.6	60.2	183	0.8	0.0/0.1/0.0	0.0/0.0/0.0
γAGNs						
Cen A Core	309.6	19.4	3.7	0.8	60.5/14.6/40.4	86.8/56.3/71.5
M87	283.7	74.5	18.5	1	15.3/7.1/29.5	9.7/12.1/23.1
NGC 1275	150.6	13.3	76	2.2	6.6/6.1/7.5	0.7/1.6/1.0
IC 310	150.2	−13.7	83	1	2.3/2.4/2.6	0.3/0.6/0.3
3C 264	235.8	73	95	0.5	0.8/1.0/0.8	0.4/1.3/0.5
TXS 0149 + 710	127.9	9	96	0.5	0.7/0.9/0.7	0.0/0.0/0.0
Mkn 421	179.8	65	136	54	11.4/48.3/14.7	1.8/19.1/2.8
PKS 0229-581	280.2	54.6	140	0.5	0.1/0.5/0.1	0.2/2.0/0.3
Mkn 501	63.6	38.9	148	20.8	2.3/15.0/3.6	0.3/5.2/0.6
1ES 2344 + 514	112.9	−9.9	195	3.3	0.0/1.0/0.1	0.0/0.0/0.0
Mkn 180	131.9	45.6	199	1.9	0.0/0.5/0.0	0.0/0.0/0.0
1ES 1959 + 650	98	17.7	209	6.8	0.0/1.7/0.1	0.0/0.0/0.0
AP Librae	340.7	27.6	213	1.7	0.0/0.4/0.0	0.0/1.3/0.0
TXS 0210 + 515	135.8	−9	218	0.9	0.0/0.2/0.0	0.0/0.0/0.0
GB6 J0601 + 5315	160	14.6	232	0.4	0.0/0.1/0.0	0.0/0.0/0.0
PKS 0625-35	243.4	−20	245	1.3	0.0/0.1/0.0	0.0/0.5/0.0
I Zw 187	77.1	33.5	247	2.3	0.0/0.2/0.0	0.0/0.0/0.0

Studying the correlation between the UHECR anisotropy and the distribution of galaxies from the 2FHL catalog (FERMI-LAT)

SBG: star burst galaxy

γAGN: γ-active galactic nucleus

UHECR: Anisotropy

[anc19]

Auger and TA

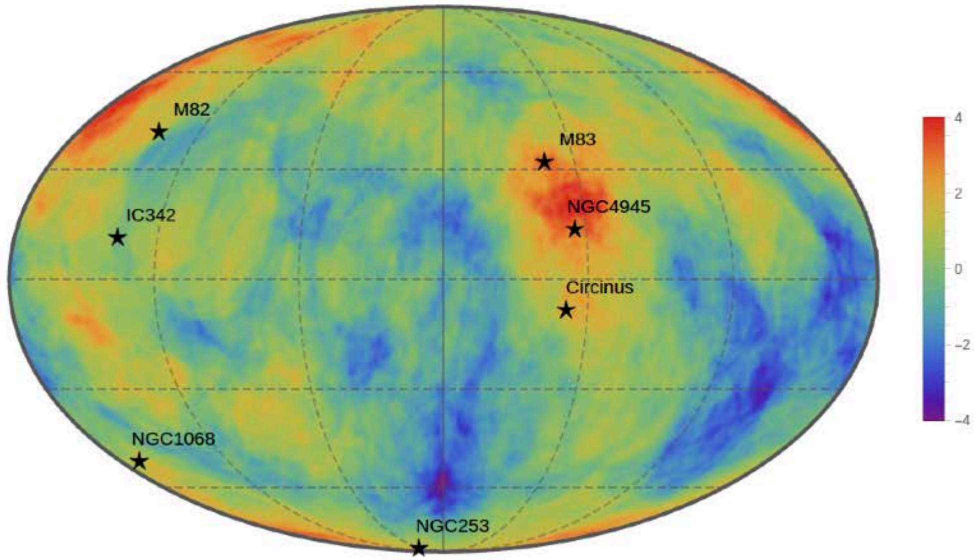

Figure 7: Skymap in Galactic coordinates of the Li-Ma significances of over-densities in 20° radius windows for 840 events recorded by Auger with $E > E_{\rm th,Auger}$ and 130 events recorded by TA with $E > E_{\rm th,TA}$. The color scale indicates the significance in units of standard deviations; negative values follow the convention of indicating the (positive) significance of deficits. Nearby SBGs providing a significant contribution to the UHECR correlation signal of Auger [3] and TA [163] are indicated by stars. From Ref. [161].

Candidate production sites

Active Galactic Nuclei

Starburst Galaxies

Auger data with a model prediction of deflection of UHECRs by galactic and extragalactic magnetic fields.

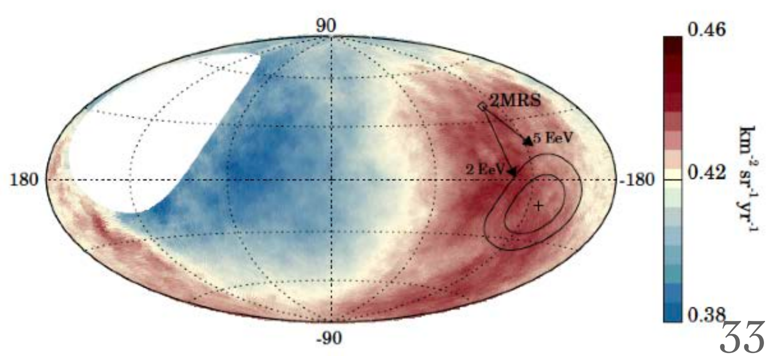

Magnetic Rigidity $\propto$ E/Z

Again the composition of UHECRs is important.

Intergalactic magnetic field is also not known well.

Energy Loss Process in Space Propagation

Greisen, Zatzepin, and Kuzmin (GZK) Cutoff

[gre66,zat66]

GZK predicted a cutoff of UHECR flux at around 10^{20} eV
due to energy-loss with the collision of CMB in extragalactic propagation

For UHECR protons

pion-production by scattering with CMB

p+photon → $\pi^{\pm}$ production

Cosmic Microwave Background (CMB)

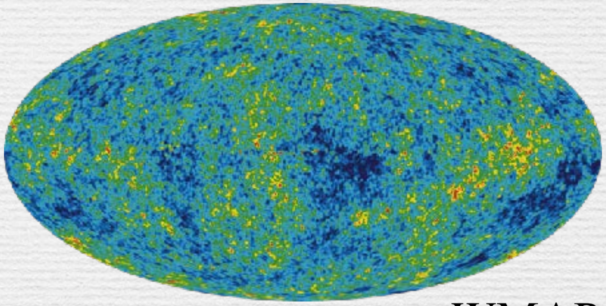

WMAP

T=2.72548±0.00057 K

For UHECR nuclei

photo-absorption of CMB

→ excitation to GDR

→ disintegration (photo-disintegration)

Energy-loss process of UHECR is a key to understood the energy distribution and composition of UHECRs and their origin, production mechanism, and the propagation.

Energy Loss Process of UHECRs in Extragalactic Propagation

[all12, kha05]

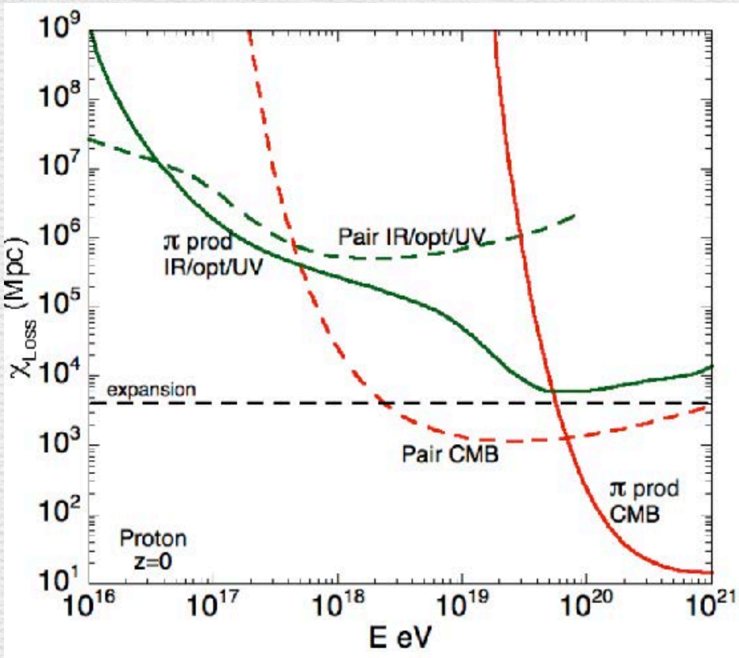

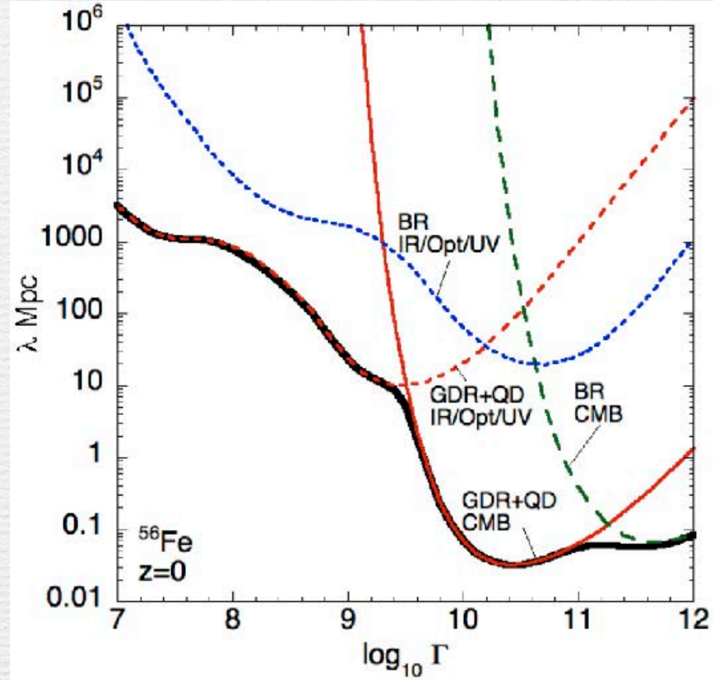

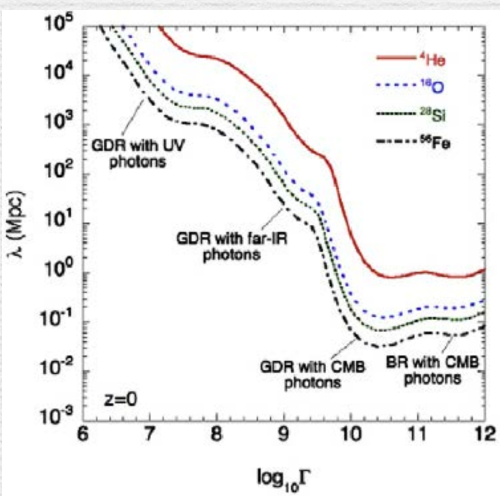

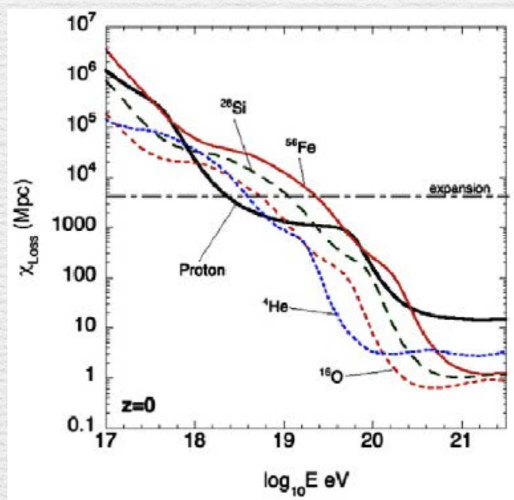

Refinements of the theoretical model in [kha05]

[ste99]

Unfortunately, photodisintegration cross section data are incomplete. For many reaction channels, $\sigma(\epsilon)$ data do not exist. Also, integrated cross section strengths are not available for all of the exclusive channels. The most complete compilation of the world's GDR cross section data exists in the 15 volumes of Fuller & Gerstenberg (1983). In these volumes GDR cross section data for ^{56}Fe, for example, are given only for the (γ, pX) channel and the inverse channels (α, γ) and (p, γ).

A Composition Reconstruction by a Model (fitted to data)

[anc19]

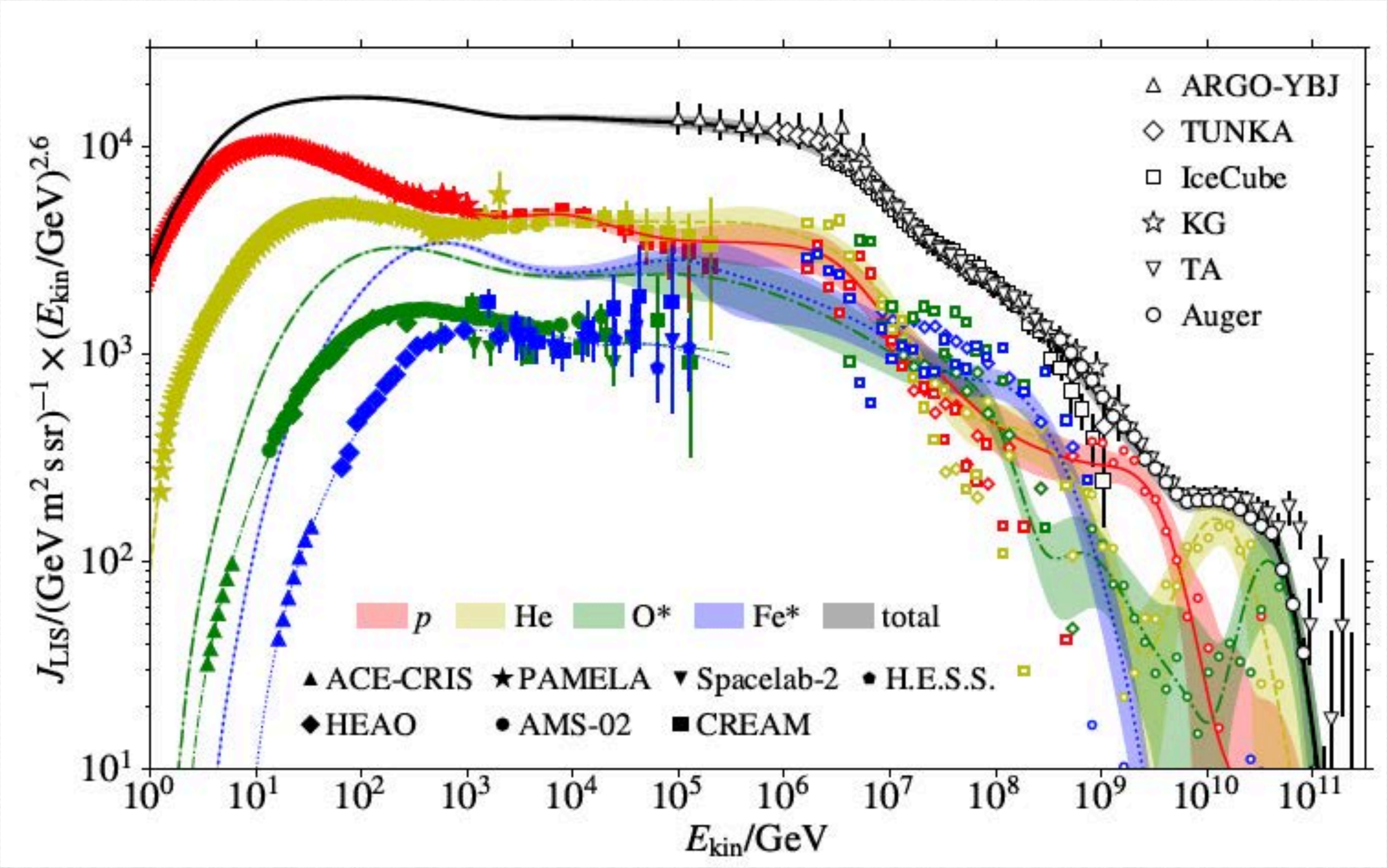

PANDORA Project

PANDORA Project

Photo-**A**bsorption of **N**uclei and **D**ecay **O**bservation for **R**eactions in **A**strophysics

Joint project among three experimental facilities with nuclear theories and astrophysical simulations

RCNP-Grand Raiden (Osaka, Japan)

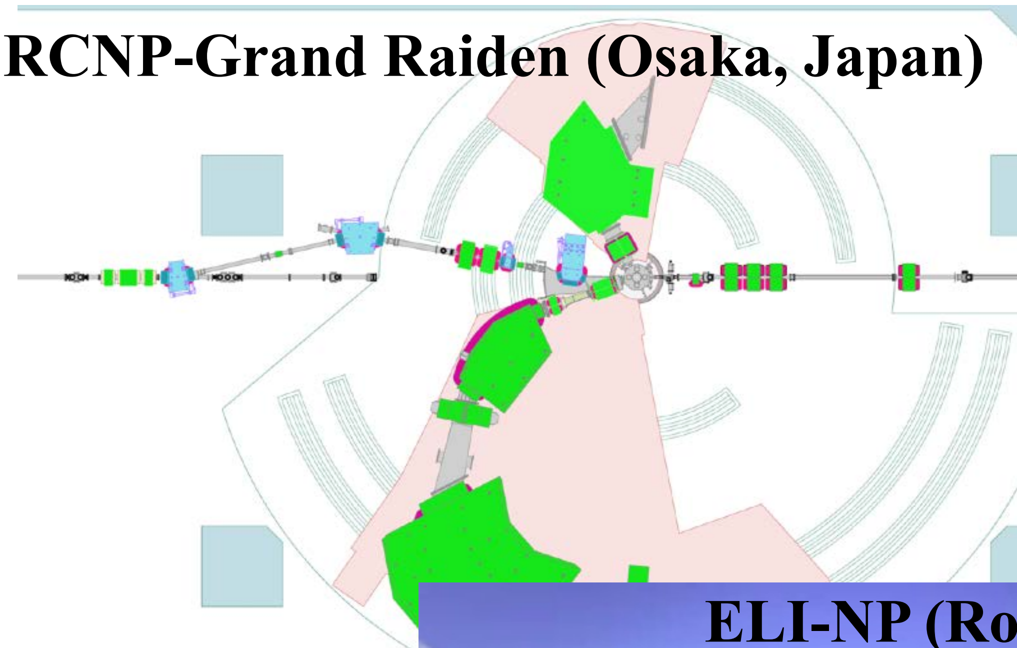

iThemba LABS South Africa

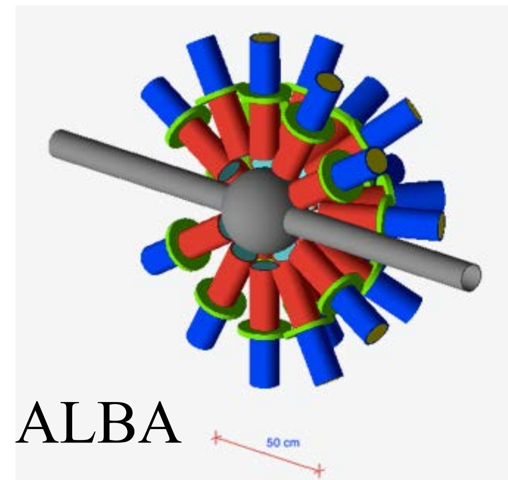

CAKE

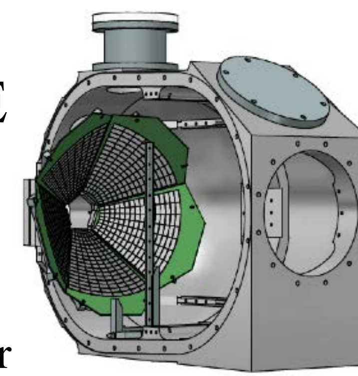

decay charge particle detector array

ELI-NP (Romania)

complementary experimental techniques

PANDORA Project

Photo-**A**bsorption of **N**uclei and **D**ecay **O**bservation for **R**eactions in **A**strophysics

Motivations

- Extragalactic propagation of ultra-high energy comic rays (UHECRs)
- Nuclear-astrophysics and nucleosynthesis
- Neutral-current neutrino detection in large volume neutrino detectors
- Nuclear Structure
  - electric dipole strength distribution: PDR, GDR, EDP
  - decay mechanism
  - gamma-decay of GR: damping mechanism
  - alpha-cluster structure

Systematic Measurement on Photo-Absorption C.S. and n,p,α,γ decays for light to A~60 stable nuclei

- photo-absorption (electric dipole) strength distribution
- n, p, α, γ decay branching ratios
- for stable nuclei from light to A~60

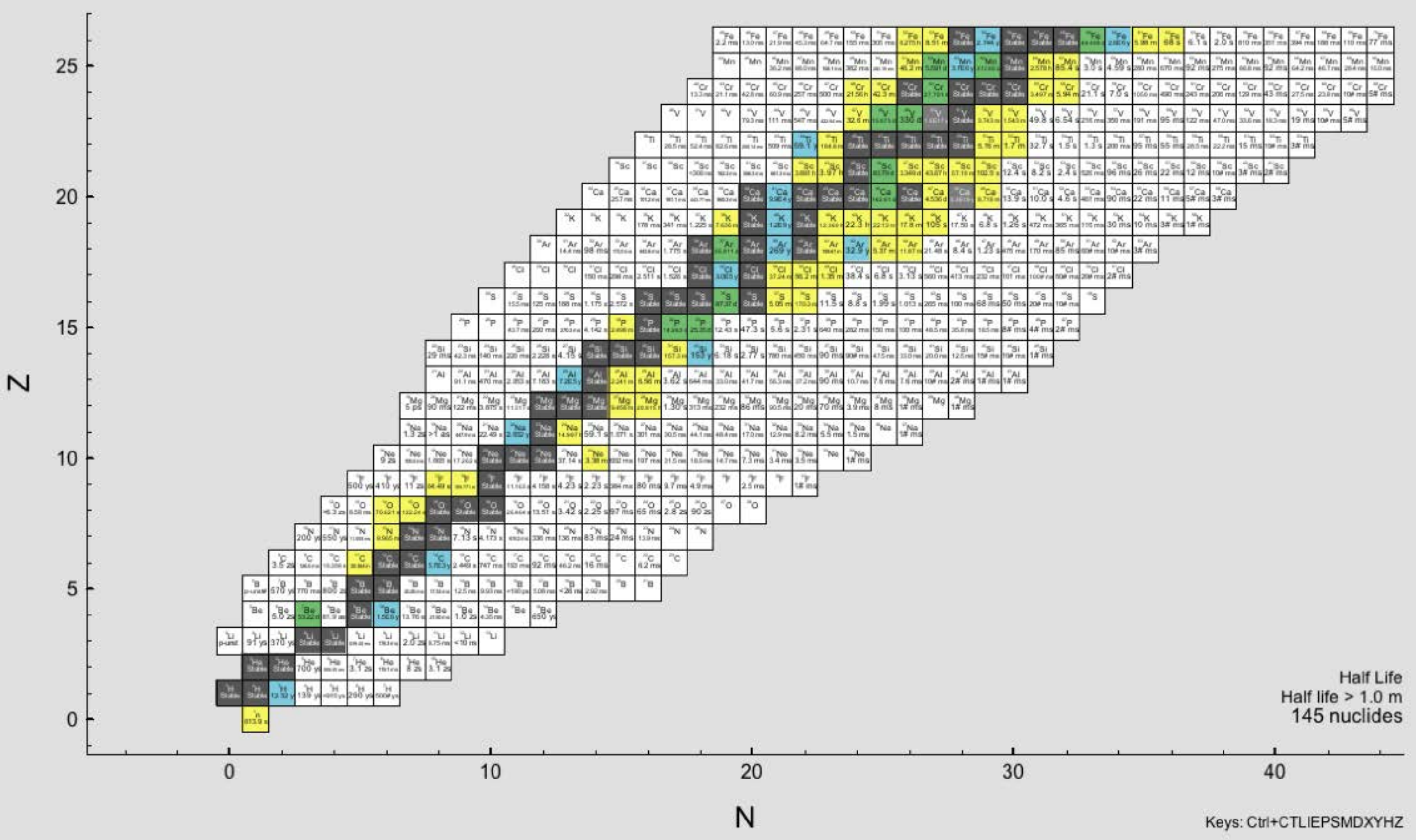

Photo-disintegration Pass of ^{56}Fe

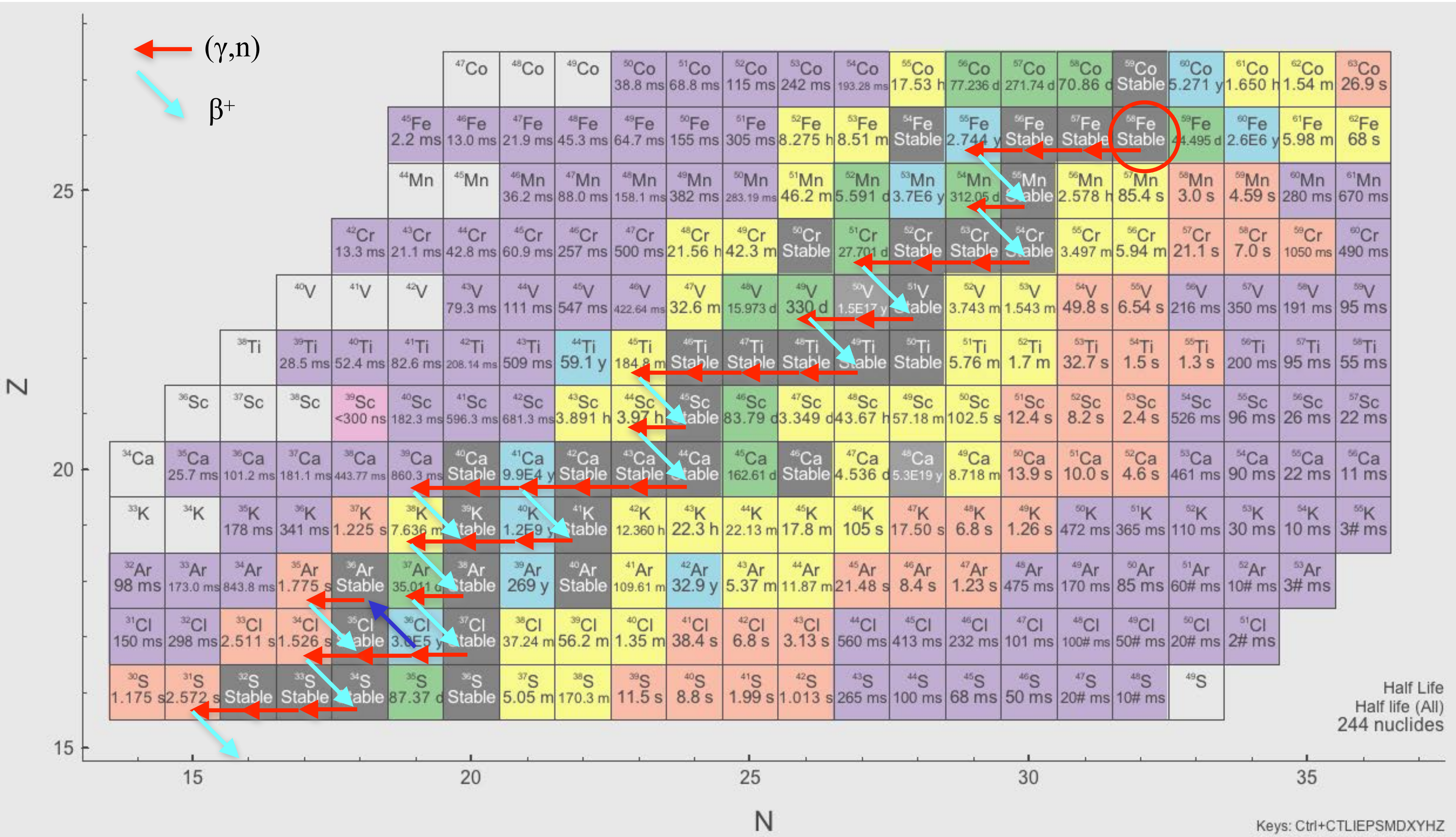

Photo-disintegration Pass of ^{56}Fe

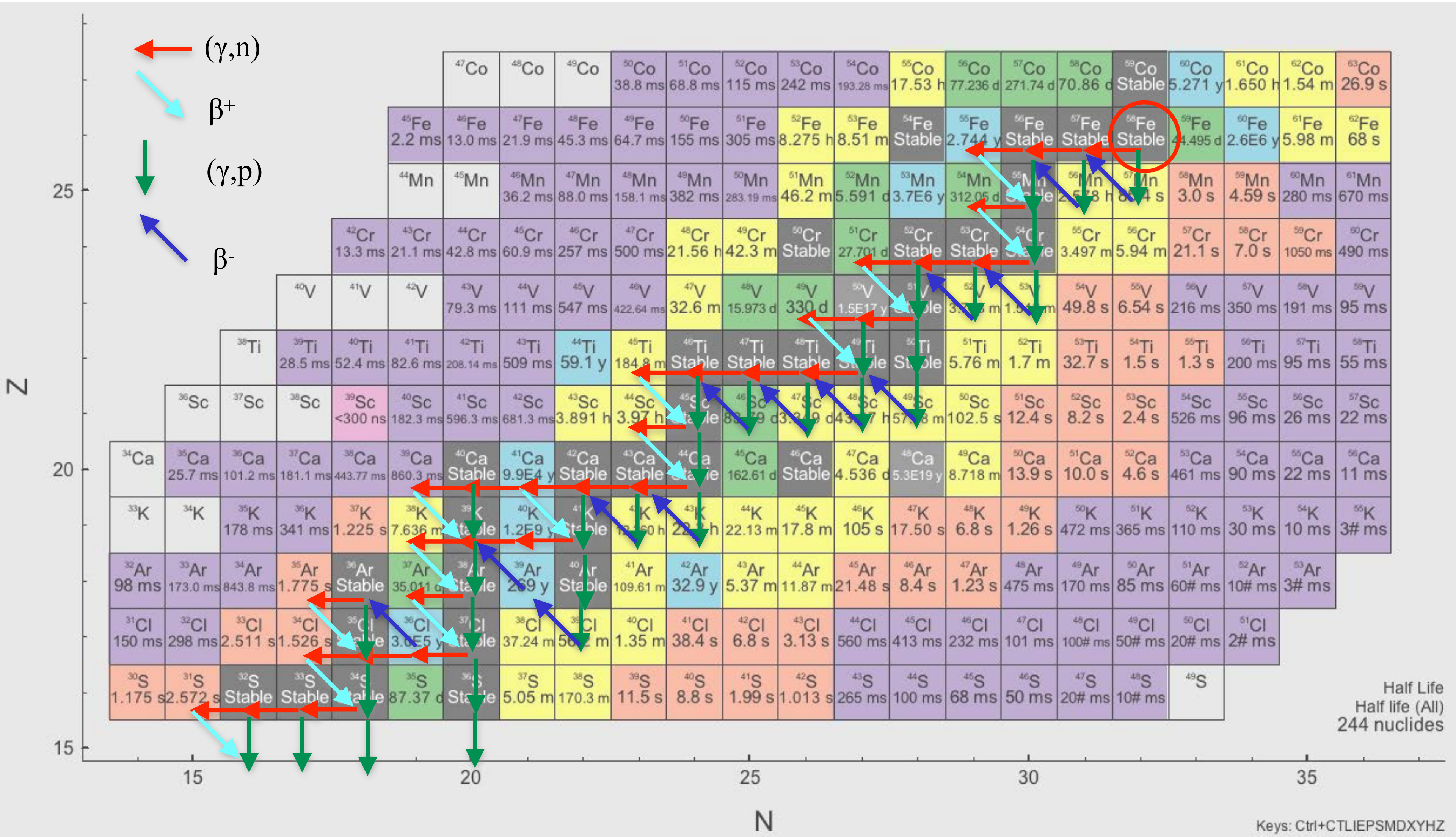

(γ,xn), (γ,α) reactions also take place.
Several unstable nuclei also contribute.

Photo-disintegration Pass of ^{56}Fe

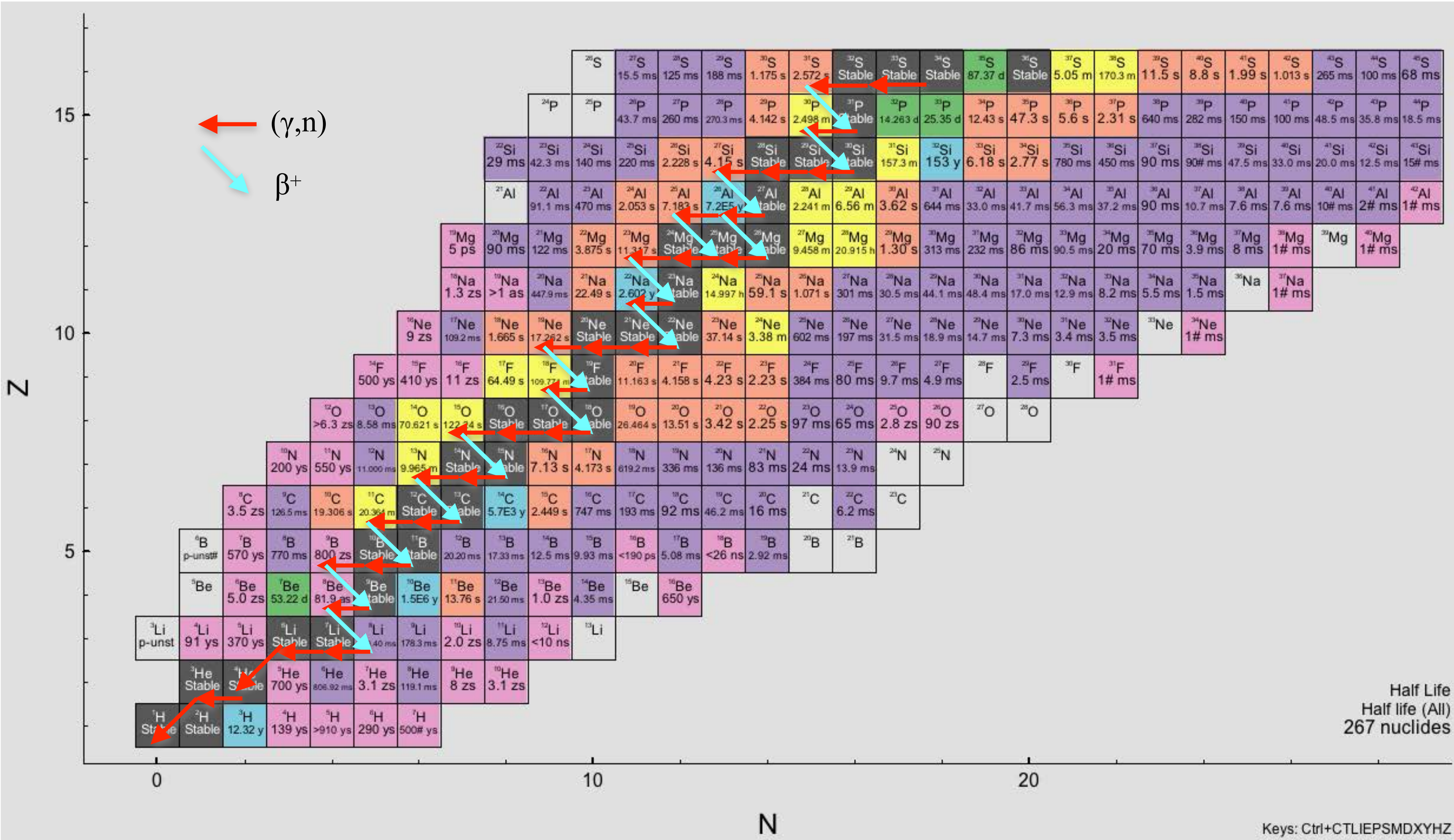

Systematic Measurement on Photo-Absorption C.S. and n,p,α,γ decays for light to A~60 stable nuclei

difficulties in theoretical modeling of light-medium mass nuclei

- stronger shell structure effects than heavy nuclei
- many-nucleon correlations: α-clustering, *np*-pairing, deformation, …
- isospin selection rule, often unimplemented in statistical calculations, e.g. in
  A(N=Z, I=0)+γ ⟶ GDR (I=1) $\not\longrightarrow$ A-4(N=Z, I=0) + α(I=0)
- Preequilibrium component of the decay

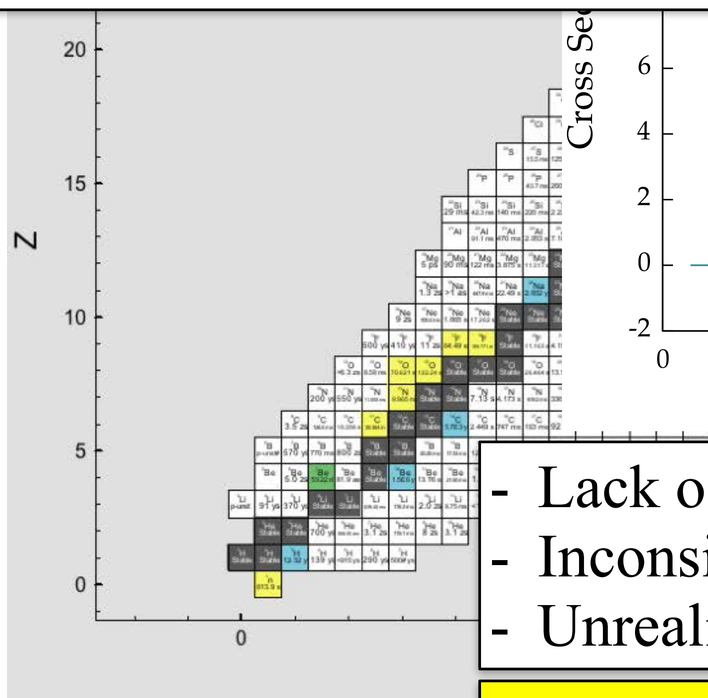

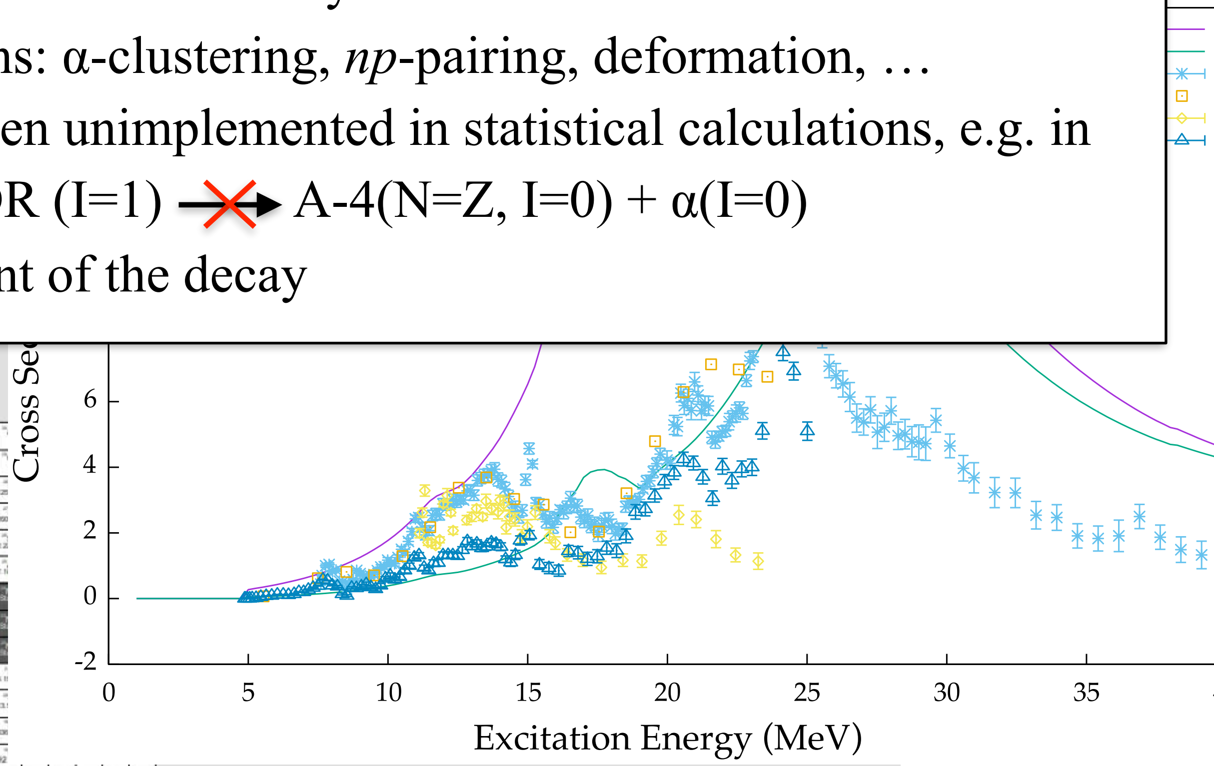

- Lack of data especially for charged particle decays
- Inconsistency among experiments
- Unrealistic predictions by models

We need good systematic data and reliable models!

Probing Photo-Nuclear Response of Nuclei

Virtual photo excitation by proton scattering

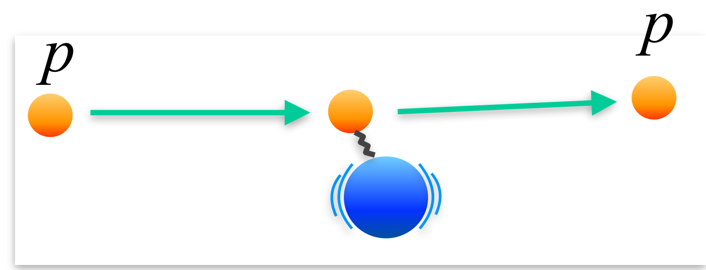

- Missing mass method
  with proton Coulomb excitation

- better for total strength
  and strength distribution
  higher cross sections
  also applicable for p,α,γ decays

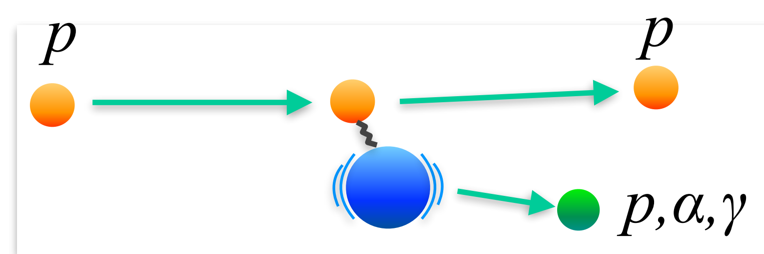

Real photo excitation

- Gamma-beam by laser-Compton
  scattering with an electron beam

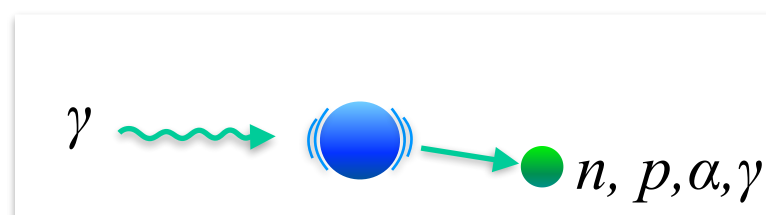

- individual decay channels
  better for absolute normalization
  applicable also for *n* and *xn* decays in addition to p,α,γ

High-Resolution Spectrometer Grand Raiden in 0-deg mode

Coulomb excitation by
proton scattering
at very forward angles

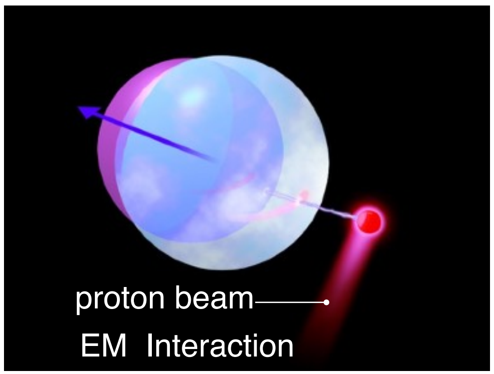

High resolution of 20-30 keV:
dispersion matching.

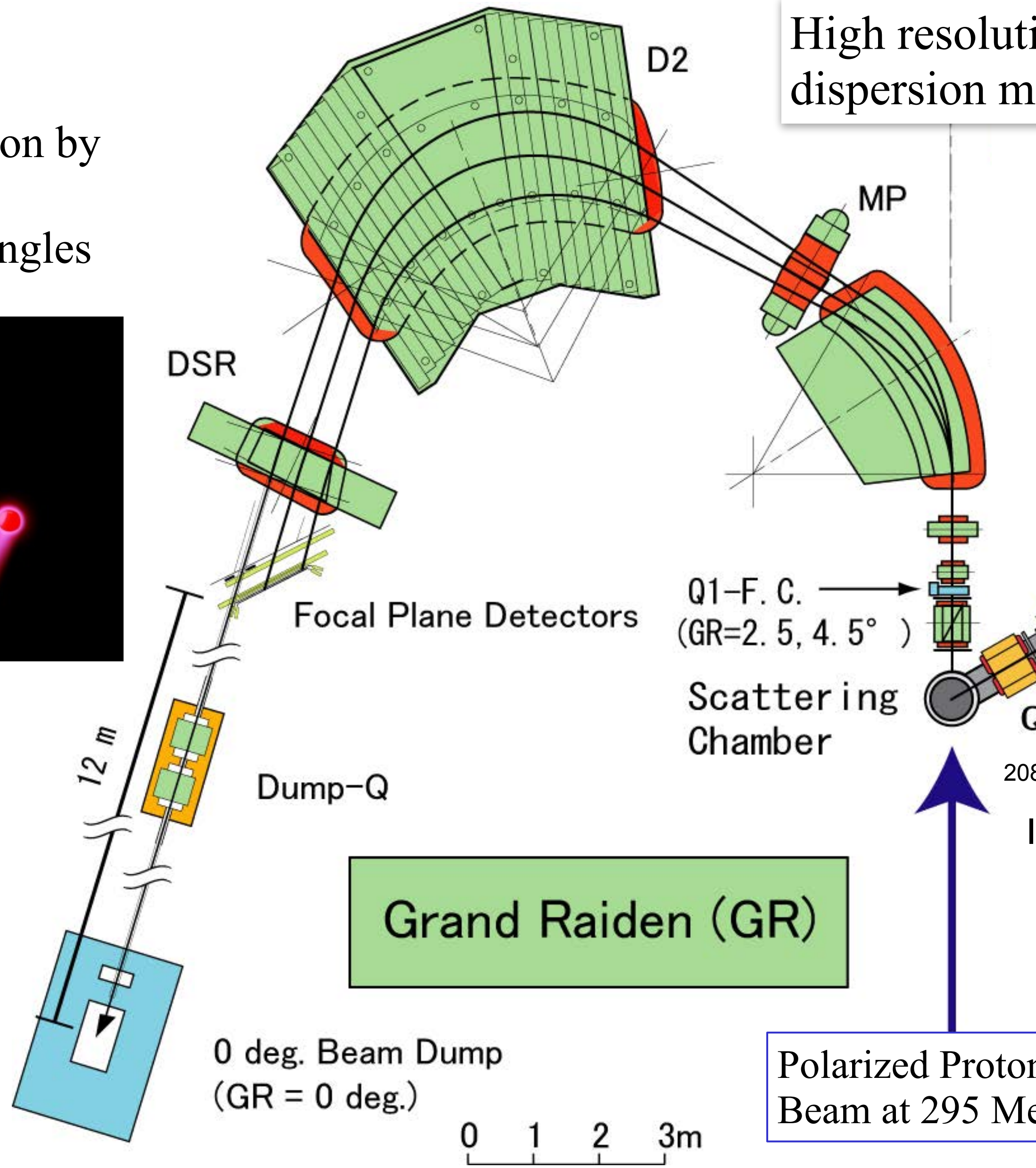

^{208}Pb target: 5.2 mg/cm^2
Intensity : 1-8 nA

Polarized Proton
Beam at 295 MeV

AT et al., NIMA605, 326 (2009)

Probing the E1 Response

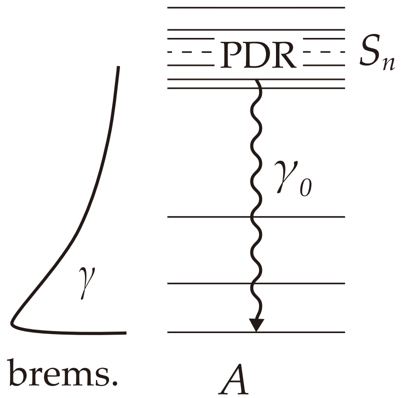

NRF with a brems. γ-beam

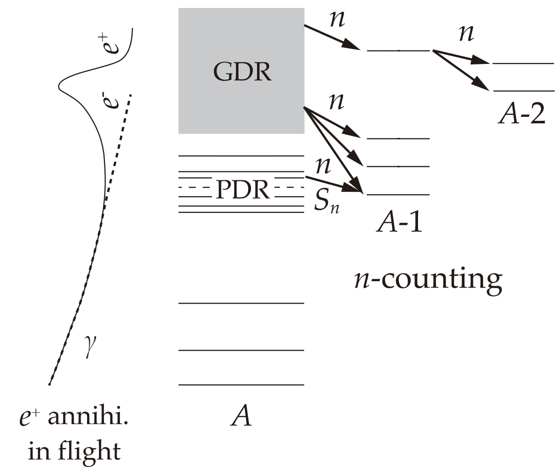

n-counting with e+ annihi. in flight

Historical Methods

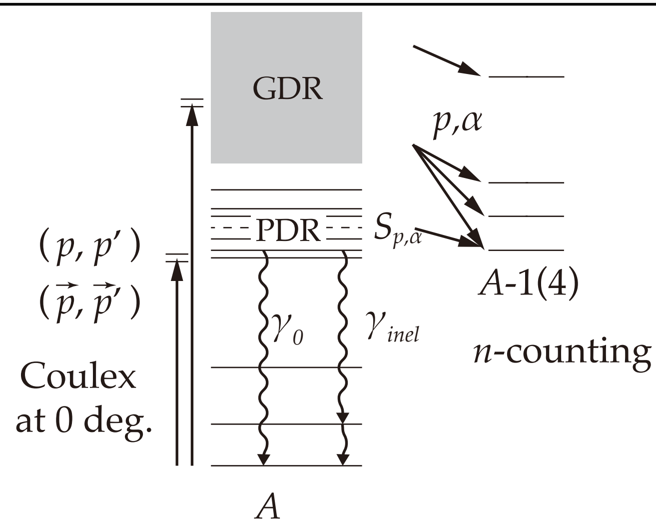

p-Coulex and decay coincidence

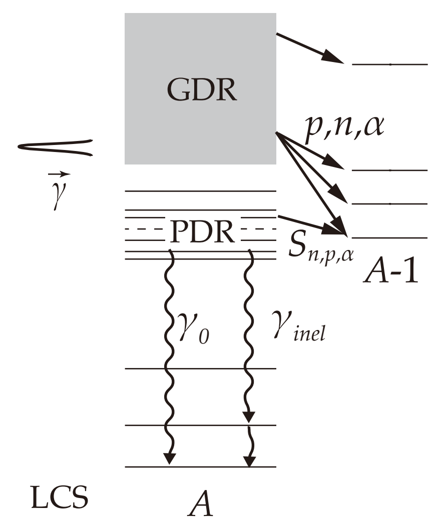

LCS-γ-beam with decay detection
high-res. high-intensity

New Methods

A. Bracco, E.G. Lanza, AT, PPNP **106**, 360 (2019)

Gamma Beam System – Layout

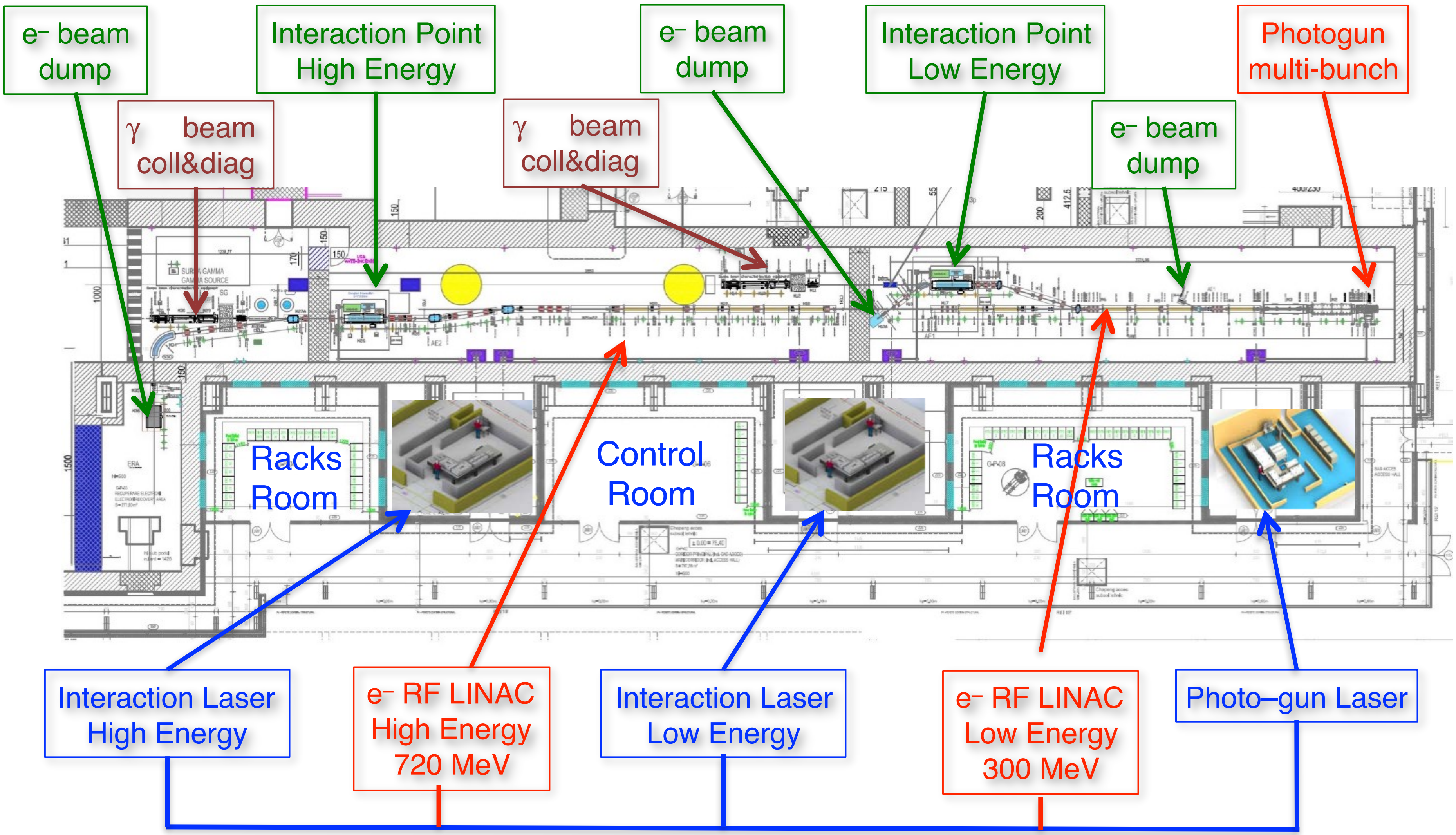

Master clock synchronization @ < 0.5 ps

High-Energy Stage: γ rays up to 19.5 MeV

Low-Energy Stage: γ rays up to 3.5 MeV

ELI-NP

K.A. Tanaka et al., Matter and Radiat. Extremes 5, 024402 (2020)

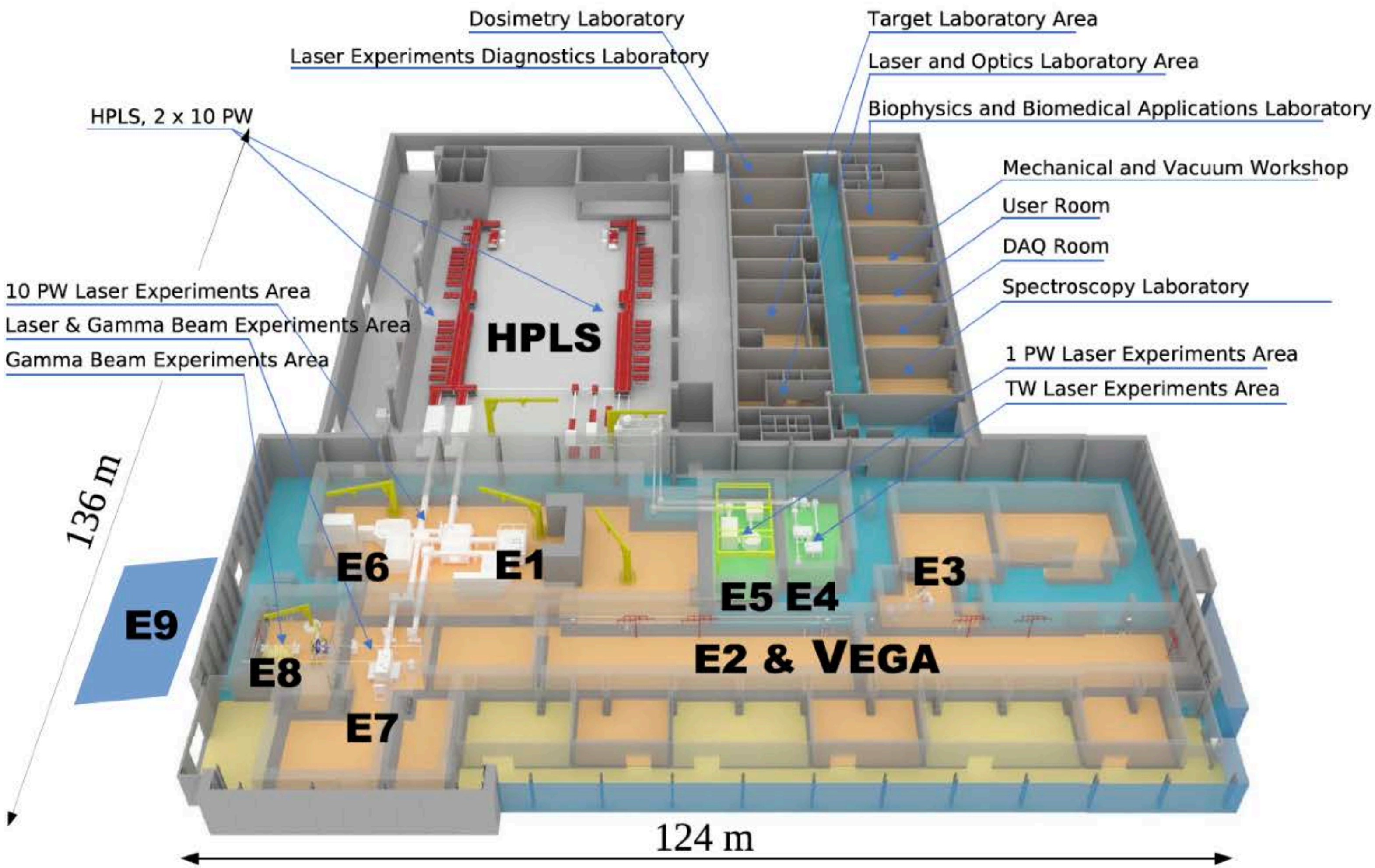

FIG. 1. Schematic overview of the HPLS and the VEGA system and associated target areas at ELI-NP. The two laser arms are depicted in red. The target areas E1, E4, E5, E6, and E7 show the 3D CAD designs of the target chambers currently under construction. The positions of the target areas E3, E8, and E9 associated with the VEGA system are indicated. The E9 area sits in the newly installed annex sketched by the blue footprint adjacent to the left side of the main building. The target area E2 will be facilitated for VEGA system-related experiments in the future.

Experiment combining three complementary facilities

Virtual Photon Exp.

RCNP 2022-

Total strength distribution up 32 MeV

γ-decay

multipole decomp. analysis (ang. dep. and polarization transfer)

iThemba LABS 2021-

Total strength distribution up 24 MeV

p,α,γ-decays

multipole decomp. analysis (ang. dep.)

Real Photon Exp.

ELI-NP 2023-

absolute c.s.

model independent separation of E1 and M1

n,p,α,γ-decays up to 20 MeV

Experiment combining three complementary facilities

Virtual Photon Exp.

RCNP 2022-

Total strength distribution up 32 MeV

γ-decay

multipole decomp. analysis (ang. dep. and polarization transfer)

iThemba LABS 2021-

Beam time approved for the first cases: ^{12}C, ^{27}Al
σ_{abs} and p,α,γ decays

Total strength distribution up 24 MeV

p,α,γ-decays

multipole decomp. analysis (ang. dep.)

Real Photon Exp.

ELI-NP 2023-

absolute c.s.

model independent separation of E1 and M1

n,p,α,γ-decays up to 20 MeV

Good systematic data
Consistency among three facilities
Reference target: ^{27}Al.

PANDORA Project: Organization

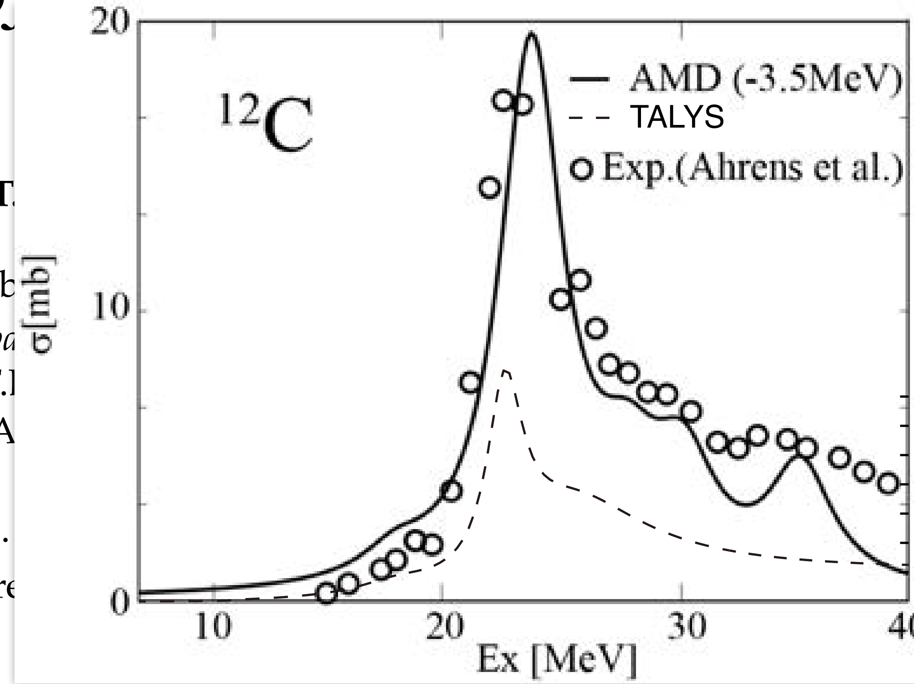

Nuclear Experiments

RCNP	*Osaka Univ.* **A. Tamii, N. Kobayashi, T.** ... ri
ELI-NP	*ELI-NP* **P.-A. Söderström**, D. Balab...
iThemba LABS	*iThemba LABS, Univ. Witwa...* **L. Pellegri**, R. Neveling, F.I... Wiedeking, K.C.W. Ki, P. A... ji, S. Jongile, A. Netshiya
TU-Darmstadt	P. von Neumann-Cosel, N. ...
U. Milano/INFN	A. Bracco, F. Camera, F. Cre...

Nuclear Theory

AMD	**M. Kimura, Y. Taniguchi**, H. Motoki	Antisymmetrized Molecular Dynamics
NRFT	**E. Litovinova**, P. Ring, H. Wibowo	Nuclear Relativistic Field Theory
RPA/DFT	**T. Inakura**	
TALYS	**S. Goriely**, E. Khan	

日本物理学会シンポジウム
「軽中重核の電弱励起・崩壊と宇宙物理」
2020年9月17日13:30-17:15

UHECR Theory

Propagation and production	**D. Allard**, B. Baret, I. Deloncle, J. Kiener, E. Parizot, V. Tatischeff **S. Nagataki**, E. Kido, J. Oliver, H. Haoning

NC Neutrino Detection

M. Sakuda, M.S. Reen, Y. Koshio,

Targets

Measurements on 10-20 nuclei in 5-10 years
with theoretical model developments

Candidate target nuclides

• ^{12}C, ^{16}O, and ^{27}Al	first cases, alpha decay, reference target
• ^{6}Li, ^{7}Li, ^{9}Be	light nuclei
• (^{20}Ne), ^{24}Mg, ^{28}Si, ^{32}S, (^{36}Ar), ^{40}Ca	N=Z nuclei, α-cluster effect, deformation
• ^{26}Mg, ^{48}Ca, ^{56}Fe	N>Z nuclei
• ^{13}C, ^{14}N, ^{51}V	odd and odd-odd nuclei
• (γ,xn) on ^{18}O, ^{48}Ca, ^{64}Ni	

Sensitivity test and selection of important nuclei are under discussions.

Summary

- PANDORA is a joint project combining complementary experimental facilities of real and virtual photon scatterings, nuclear theories and astrophysical simulations. Measurements will start in 2021.
- Systematic measurements on photo-absorption cross sections and *n*,*p*,α and γ decays from light to A~60 nuclei are planned.
- Development of theoretical models is planned by AMD, RPA and RNFT.
- We appreciate your suggestions and support from the community.

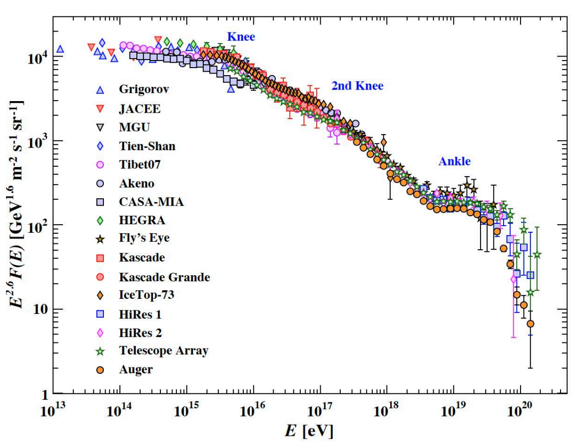

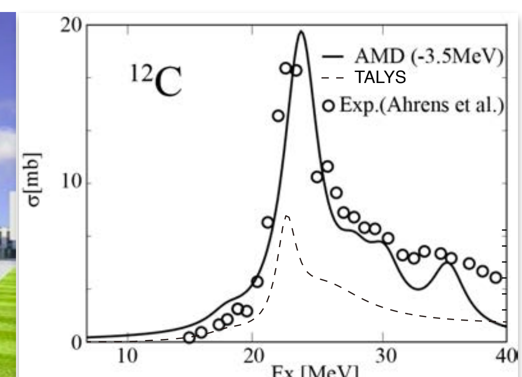

References

References:

reviews:

[anc19] L.A. Anchordoqui, Phys. Rep. **801**, 1(2019).

[mol18] S. Mollerach and E. Roulet, Prog. in Part. and Nucl. Phys. **98**, 85 (2018).

[daw17] B.R. Dawson, M. Fukushima and P. Sokolsky, Prog. Theor. Exp. Phys. 2017, 12A101.

articles:

[aab14] A. Aab et al., Phys. Rev. D **90**, 122006 (2014).

[aab15] A. Aab et al., Astrophys. J **804**, 15 (2015).

[aab18] A. Aab et al., Astrophys. J. Lett. **853**, L29 (2018).

[abb18] R.U. Abbasi et al., Astrophys. J. **862**, 91 (2018).

[abb19] R.U. Abbass et al., Phys. Rev. D **99**, 022002 (2019).

[abu12] T. Abu-Zayyad *et al.*, Nucl. Instrum. and Methods in Phys. Res. A **689**, 87 (2012).

[all12] D. Allard, Astropart. Phys. **39-40**, 33 (2012).

[ast19] ASTRO2020 Science White Paper, arXiv:1903.04063v2 [astro-ph.HE]

[aug04] Auger Collaboration, Nucl. Instrum. and Methods in Phys. Res. A **523**, 50 (2004).

[aug15] The Pierre Auger Collaboration, Nucl. Instrum. and Methods in Phys. Res. A **798**, 172 (2015)

[aug15b] The Pierre Auger Collaboration, arXiv1604.03637 [astro-ph.IM].

[aug17] The Pierre Auger Collaboration, Science **357**, 1266 (2017).

[gor18] D. Góra, Universe **2018**, 4, 128.

[gre66] K. Greisen, Phys. Rev. Lett. **16**, 748 (1966).

[kha05] E. Khan et al., Astropart. Phys. **23**, 191 (2005).

[ste99] F.W. Stecker and M.H. Salamon, Astrophys. J **512**, 521 (1999).

[tok11] H. Tokuno *et al* J. Phys. Conf. Ser. 293, 012035(2011).

[tok12] H. Tokuno *et al.*, Nucl. Instrum. and Methods in Phys. Res. A **676**, 54 (2012).

[zat66] G.T. Zatsepin and V.A. Kuzmin, JETP Lett. **4**, 78 (1966).

[PDG2018] Review of particle physics, particle data group, Phys Rev. D **98**, 1(2018).

Thank you

for your attention